Anelastic Properties of Mild Steel

at Moderate Stresses

by

Duncan Morrison, B.Sc., A.M.I.E.S

Thesis submitted for the Degree of Ph.D.

Glasgow University.

February, 1954.

DECLARATION

The author wishes to declare that the conception and execution of the research herein described, as well as the design of the apparatus with which it was carried out, are his own work.

INDEX

Summary.

This thesis describes an experimental investigation of the elastic hysteresis and other non-linear effects occurring in mild steel at stresses from about 2 ton/in^2 up to the yield point. The design and construction of a new apparatus for making measurements of these quantities is also described.

An important feature of this equipment is that the absolute shape of the hysteresis loop for a bending specimen is obtained and not merely the area or strain width. Due to this feature measurements can also be made of the departure from true linearity in the stress-strain diagram of the material for a single loading.

The results obtained on a few mild steel specimens agree well with those obtained by other investigators in so far as they are directly comparable. A remarkable feature of the experimental results is that for moderate stress ranges the main curvature in the hysteresis loop occurs in the unloading part of the stress cycle. Although this is in contradiction with the tacitly accepted form of the loop it is shown that it does in fact agree with

(1) the accepted relationship between energy dissipation and stress amplitude.

(2) the observed results for the deviation from true linearity in a single loading.

(3) the hypothesis that elastic hysteresis is due to plastic flow occurring at numerous discontinuities in the bulk of the material.

A mathematical section deals with the problem of determining the damping coefficient of a uniformly stressed material from the experimental results obtained on a specimen having an arbitrary stress distribution.

Since the preparation of this thesis a description of the apparatus together with some preliminary results has been published in Engineering p.141, Volume 177, (1954).

1.1 Historical review.

Damping capacity or elastic hysteresis, by which we mean that property whereby a metal dissipates mechanical energy when subject to stress fluctuations, has been studied by engineers and physicists since the middle of the last century. The first major paper on the subject is probably that of Lord Kelvin (1)*, given in the Proceedings of the Royal Society, Vol. 14, 1865. The discovery of fatigue phenomena in metals stimulated a great deal of research on damping capacity since it was recognized that a machine part having a high damping capacity would incur lower stresses when running through a critical speed. Secondly, it was hoped that studies of damping capacity would elucidate the nature of the fatigue process and possibly provide a rapid method of determining the endurance limit of materials. This work - carried on from about 1890 to 1920 - was only partially successful in its main objectives, but yielded a great deal of information on damping capacity itself. This period also produced the basic experimental techniques for the measurement of damping capacity, with the obvious exception of those involving electronic methods.

Since about 1920 damping research has proceeded on two complementary lines dealing with low stresses (up to say 100 lb/in^2.), and moderate stresses (up to near the yield point of the material) respectively.

1.2 Damping capacity at low stresses.

Damping capacity at low stresses has been studied on a physical basis notably by Zener (16) and his co-workers.

* Numbers in parentheses refer to bibliography on page 52

It is found that damping can be related to various relaxation processes - thermal, magnetic, etc. If, for example, a tensile load is applied to a rod the resultant increase in length is accompanied by a fall in temperature and if the load is maintained a further increase in length will occur when the temperature of the rod again rises to room temperature. Applying this reasoning mathematically to the case of an alternating load leads to the result that the alternating extension lags slightly behind the load thus giving rise to the damping effect.

A significant feature of this type of damping is that the damping coefficient - the proportion of the maximum strain energy dissipated during each stress cycle - is independent of the stress amplitude and dependent on the stress frequency.

1.3 Damping capacity at moderate stresses.

Results, very different from those quoted above, have been obtained in investigations of damping capacity at moderate stresses. In this stress region it is found that the damping coefficients are highly dependent on the stress amplitude, and practically independent of the stress frequency. Dorey (9) found damping coefficients varying by as much as the eighth power of the stress amplitude. Rowett (3) found agreement between the results of static experiments and those carried out at over 2000 c.p.m., but it should be noted that the correspondence of two tests at different frequencies - and a static test does have a real frequency however low - does not necessarily prove the damping coefficient to be independent of frequency. Reference to the frontispiece in Zener's book shows that a plot of damping coefficient v frequency has many peaks and valleys when the damping coefficients due to various relaxation processes are considered and thus similar

coefficients could be obtained at widely different frequencies.

These points of difference between damping effects at low and at moderate stresses have been dealt with in a recent report by Linacre (17). The work described in this thesis is confined to considerations of the damping effects occurring in mild steel at moderate stresses and at room temperature.

2.1 The measurement of damping capacity.

Before considering the various methods which have been devised for the measurement of damping effects it is important to estimate the general magnitude of the quantities concerned. Figure 2.1 shows, greatly enlarged, an elastic hysteresis loop ABCD, the area of this loop representing the amount of energy dissipated per stress cycle. The damping coefficient is defined as the ratio of this energy loss per cycle to the total strain energy stored in the specimen at the instant of maximum stress,

$$\text{i.e.} \quad \text{Damping coefficient } D = \frac{\text{Loop area}}{\text{Area of } \Delta OAF}$$

Many other methods have been used for the expression of damping capacity values these being based either on the method by which, or the purpose for which, the results were obtained. It will be noticed that the coefficient D takes account of the elastic modulus and thus makes for easy practical comparisons between various materials.

As regards magnitude of the hysteresis loop we can assume for a general discussion that D will be of the order 0.01. Common values for steel range from about 0.001 up to possibly 0.1 at high stresses near the yield point.

For an estimate of the dimensions of the loop consider

a steel sample subjected to an alternating tensile stress of ± 20,000 lb/in.^{2} and having D = 0.01 as assumed above.

Total strain energy at instant of maximum stress $= \frac{f^2}{2E}$

$= 6.66$ lb.in/in.^{3}

$\therefore$ Energy dissipation per cycle = loop area

$= D \times 6.66 \fallingdotseq \underline{0.07}$ lb.in/in.^{3}

The stress difference at zero strain, Δf, can be estimated by taking the sides of the loop to be approximately parabolic in shape.

Then loop area $= 2/3 \times \Delta f \times 2\epsilon_m$

$= D \times \frac{1}{2} \times \epsilon_m \times f_m$

$$\frac{\Delta f}{f_{max}} = \frac{3}{8} D$$

For the case considered

$$\Delta f = \frac{3}{8} \times 0.01 \times 20{,}000 = \underline{75 \text{ lb/in.}^2}$$

And it follows that $\Delta\epsilon$, the strain difference at zero stress $= \frac{\Delta f}{E} = \frac{75}{30 \times 10^6} = \underline{2.5 \times 10^{-6}}$ in/in.

2.2 Variables known to affect the damping coefficient.

The damping coefficient of metals is known to be dependent on a number of variables. The more important of these are

(a) Stress amplitude:- This is probably the most important variable in the moderate stress range. Generally speaking the damping coefficient rises with increasing stress amplitude, and at high stresses this increase is very rapid.

(b) Stress history:- It is known that damping coefficients depend not only on the instantaneous stress amplitude but also on the previous stress history of the specimen.

In fatigue tests quite marked changes in damping capacity have been noted as the test proceeds, and these are not confined to the period just before fracture when the specimen gets very warm. Dorey also found an increase in damping coefficients when the specimen had previously been loaded above a critical stress.

(c) Temperature:- Like other mechanical properties such as strength, ductility etc., damping capacity varies widely with the temperature of the test specimen.

(d) Surface finish of the specimen:- Some investigators have found the damping values to be affected by the surface finish of the specimens used, highly polished specimens generally giving lower damping coefficients than those having a poorer surface.

2.3 Experimental methods for the measurement of damping capacity.

2.31 Static plotting of the hysteresis loop:-

This is probably the most obvious method of measuring damping capacities provided that we can assume the damping effect to be independent of frequency. When, however, we consider the magnitude of the hysteresis loops to be measured we find that extremely accurate - not merely delicate - apparatus would be required. Referring to our previous calculation (para. 2.1) we see that the strain width of a typical loop is only a few parts per million. Since the best mechanical and optical extensometers available have a strain sensitivity limit of about 10^{-6} the straightforward use of a normal extensometer can only give reliable indications of very large hysteresis loops such as those occurring at high stresses. It is of some interest

to note that Bairstow (2), using this method, concluded that hysteresis looping only occurred above the endurance limit of the material. These remarks also apply to the ingenious machine described by Saran (10) in which, by an arrangement of mirrors, the hysteresis loop of a torsional fatigue specimen is traced by a spot of light falling on a ground glass screen.

Rowett, (and later Dorey), used an apparatus in which the damping capacity of torsional specimens was determined by measuring the width of the hysteresis loops at various stress levels. Strains were deduced from the rotation of micrometer screws which were adjusted to give null readings on high quality spirit levels. Loads were deduced from the strain of a bar, connected in series with the specimen, and assumed to be perfectly elastic. Incidentally, this is a system which disproves the assumption, sometimes made, that the lowest of a set of damping readings is the most accurate. In the extreme case where the measuring bar was identical with the specimen no hysteresis looping would be observed.

As regards the effects of stress history this can be arbitrarily chosen in a static machine. On the other hand the usual slow operation of static machines makes them unsuitable for the applicatien of large numbers of stress cycles such as the fatigue life of a specimen.

2.32 <u>The measurement of the energy input required to maintain steady stress variations - the method of lateral deflection</u>.

The measurement of the energy required to maintain a specimen in a state of steady alternating stress offers a ready means of finding the variation in damping capacity during the fatigue life of a specimen. Probably the best

mechanical method of making this measurement is that devised by Mason (4). The principle of this method (see Fig. 2.32) is that during a Wohler fatigue test the loading bearing is displaced transversely as well as vertically from the axis of rotation of the driving chuck. This displacement t is such that

Damping work done on specimen per revolution

$$= 2\pi F \times t$$

Recent papers by Lazan and Lazan and Wu (18) describe a modification of this method overcoming some of the experimental difficulties. They have obtained interesting data on the variation of damping capacity and effective modulus of elasticity during the fatigue life of mild steel specimens.

2.33 Calorimetric methods. The measurement of the heat produced by a specimen subjected to a steady alternating stress provides a method for the determination of damping capacities. It is, however, questionable whether all the damping work done on the specimen is transformed into heat, particularly near the beginning of a test run when the damping coefficient is known to vary with the number of cycles of stress. In addition if, to facilitate measurement, the specimen is allowed to become warm the temperature change may influence the results obtained.

2.34 Vibration decay methods. The most widely used method of damping capacity measurement is probably that based on observations of the rate of decay of mechanical vibration of a system in which the specimen is the main elastic member. A commercial apparatus has been produced for carrying out tests of this type (12).

A serious disadvantage of this method is that the stress history of the specimen cannot be arbitrarily chosen

amd this limits the use of this method for fundamental research other than in the low stress range.

3.1 Apparatus developed during the present research.

If we examine the various methods of damping measurement outlined in Section 2 we find that while all are capable of giving information on the area of the hysteresis loop, i.e. the energy dissipated per cycle, none are capable at moderate stresses of giving observations of the loop shape. Rowett's results are often referred to as determining the loop shape but his observations are of loop widths at various stress levels which are then assumed to lie symmetrically on either side of an elastic line.

It is felt that observations of the true shape of the hysteresis loop could help in an understanding of the nature of the damping process and the ability to make observations of this kind is the main feature of the apparatus developed in the present research. In addition this apparatus permits the measurement of the small departures from true linearity which occur in the nominally elastic portion of the stress strain diagram of a steel specimen during a single static loading.

Basically the loop shape is found by plotting statically observed points. The chief disadvantage of the equipment is its slowness of operation, about one minute being required for each plotted point and this amounts to about 10 minutes per cycle of stress if reasonable accuracy of shape is to be attained. The specimen used is subjected to a uniform bending moment and the order of accuracy is such that non-linearities in the stress strain diagram of as little as 1 lb/in^2 are detectable.

3.2 Basic principles of operation. The main elements of the apparatus used are shown in Fig. 3.2.1. A specimen A

subjected to a bending action is clamped at its lower end to a rigid base. Rigidly clamped to the upper end of the specimen is a heavy inverted pendulum B, having a weight W effectively concentrated at a distance y from the mid-point of the specimen. The whole system is deflected to an angle θ from its initial vertical position by the application of an external moment m.

Considering the static equilibrium of the system we see that

Resisting moment of specimen = Total clockwise moment on pendulum

$$= Wy \sin\theta + m$$

also

Resisting moment of specimen = Linear part proportional to θ + non-linear parts giving hysteresis, creep, etc.

$$= k\theta + F(\theta)$$

where k = nominal flexural stiffness of specimen (lb.in/rad)

$F(\theta)$ = non-linear function of θ which is to be determined.

Inserting these values in the original equation

$$k\theta + F(\theta) = Wy \sin\theta + m$$

and if we replace $\sin\theta$ by θ

$$m = (k - Wy)\,\theta + F(\theta) \quad \ldots\ldots\ldots\ldots\ldots \quad (1)$$

By arranging $Wy \simeq k$ we can reduce the linear part of the resisting moment equation to a very small proportion of its original value. $F(\theta)$ however, remains unchanged in magnitude and thus observations of m contain the function $F(\theta)$ as a first order quantity. The assumption $\theta = \sin\theta$ is valid for small values of θ. For larger values the error involved is easily calculable.

As an example consider a specimen having a stiffness k of 100 lb.in/radian, deflected through an angle $\simeq$ 0.01 radians

?

and having a damping coefficient D of 0.01. The peak moment on the specimen is 100 x 0.01 = 1 lb.in. and proceeding as in para. 2.1 the moment difference Δm at zero deflection is 0.00375 lb.in. Thus in a straightforward stress-strain test we should have to measure accurately - to say 1% - a quantity slightly less than 2/1000 of the full deflection range.

If, however, this specimen is set up in the apparatus outlined above with Wy adjusted to 99.5 lb.in. - a value quite easily attained in practice - the maximum applied moment m would be reduced to (100 - 99.5)0.01 = 0.005 lb.in. The moment difference Δm would remain unchanged and the complete diagram of m v. θ is shown in Fig. 3.2.2 in which the hysteresis loop is a prominent part of the figure.

As regards measurement of the hysteresis loop the moment m will be much smaller than the full moment applied to the specimen but on the other hand the relative accuracy of measurement need not be exceptionally high.

3.3 Leading dimensions of apparatus.

The basic dimensions of an apparatus of this type are those of the pendulum and specimen. If the specimen is small it will be difficult to machine and in addition the moment m will be very small indeed. If on the other hand the specimen is large the pendulum would also have to be large and consequently difficult to handle. This is of some importance as it is desirable to mount the pendulum by hand after the specimen has been inserted in the apparatus.

A 1" square steel bar about 4 feet long was used for the pendulum and this together with an adjustable bob weight gives a value of about 500 lb.in. for the product Wy, thus fixing a flexural stiffness of about 500 lb.in/radian for the specimen. In addition the specimen should also satisfy

the conditions that

(1) the effective length is small compared with the length of the pendulum. This ensures uniformity of the bending moment along the specimen,

and (2) in a steel specimen a reasonably high bending stress - say 20 tons/in^2 - can be attained with a small angular deflection - say 0.05 radians.

These various conditions are satisfied by the specimen shown in Fig. 3.3. The "working section" is 2" long and a 2" length of uniform rectangular section is left at each end for clamping.

3.4 General description of complete apparatus.

The upper frame-work and working parts of the apparatus are shown in Plate 1. This upper frame is supported on levelling screws which bear on a lower structure bolted to the concrete floor. Both the upper and lower frames are built up from standard rolled sections with welded joints throughout.

The lower end of the specimen is clamped to a pillar welded into the upper frame. The upper end of the specimen is clamped to a block carrying a horizontal arm which was used during the development of the apparatus. The pendulum is also clamped to this block - clamping at this point being effected by a screw - operated cam.

3.51 Load and strain measurements.

The measurement of the pendulum deflections and of the associated small moments m has proved by far the most difficult part in the development of this equipment. Several different systems (described briefly in Section 7) were tried and found unsatisfactory, but these preliminary attempts gave an indication of the requirements of a suitable load and deflection measuring system, which are as follows:-

(1) The total range of moment m required is about 0.2 lb.in. and if possible readings should be accurate to about 1/500th part of this.

(2) Observations must be based on applying arbitrary deflections to the pendulum and then measuring the required moment m by some form of comparatively stiff spring balance. This is the only system which will operate satisfactorily when as in Fig. 3.51.1 the m.v. e hysteresis loop has sections in which $\frac{dm}{d\theta}$ is negative.

(3) The load measuring system must be self indicating without the necessity for null method adjustments since creep effects may be encountered making it impossible to obtain steady null readings.

These requirements are met by the arrangement finally adopted and shown in Fig. 3.512 and Plate 2. The swinging plate P in Fig. 3.512 is carried on a pivot arranged in line with the mid-point of the unstrained specimen, and can be deflected by known amounts by the micrometer screw M. The pendulum is coupled to plate P by a load measuring unit U. If we consider U for the time being as simply a sensitive and stiff spring balance then the pendulum deflection will be practically the same as that of the plate, as given by the micrometer reading, and the load readings on U will be proportional to the moment m required on the pendulum. The maximum linear movement required at the load point will be approximately $\pm$ 0.05 radians angular deflection x 12" radius = $\pm$ 0.6". Thus by the phrase "stiff spring balance" we shall have to mean a balance having a total deflection under load of only a few thousandths of an inch in order that the assumed equality between the pendulum deflection and that of plate P shall hold good.

3.52 Simple pneumatic load measuring unit.

The first load measuring unit tried which gave any real promise of satisfactory operation was the simple pneumatic unit shown in Fig. 3.52. Air from a supply at about 4 lb/in^2. is fed through a choke to a small sharp-edged jet fixed to plate P and impinges on the surface of the pendulum bar. Provided the gap g between the jet edge and the pendulum is small compared with the jet diameter than the force exerted on the pendulum is simply the product of the jet pressure p and the jet area. Pressure p is indicated on a simple water manometer.

A further study of Fig. 3.52. shows the system to be statically self balancing. If pressure p is too large then the pendulum will move to the right opening the gap g. Due to the influehce of the choke in the air supply line this will cause a decrease in pressure p the process continuing until balance is attained. By using a small diameter choke the decrease in pressure can be related to a very small increase in gap g.

The whole arrangement is inherently sensitive. Using a jet 5/32" dia. then for a pressure change of 1 lb/in^2. the corresponding load change is $\frac{\pi}{4}\left(\frac{5}{32}\right)^2 = 0.024$ lb. The corresponding water manometer reading would be about 28" giving a sensitivity of less than 0.001 lb. per inch reading on the manometer.

In practice this simple system was found unsatisfactory due to the occurrence of dynamic instability. This effect, which arises from the inevitable time lag between the change in gap g and the corresponding pressure change, gives rise to continuous violent oscillation of the whole system making observations impossible.

The most obvious method of overcoming this condition

is by fitting a viscous damping device to the pendulum. This was tried, and a fair number of loops plotted but the dashpot required was so heavy (3" dia. piston, 0.1" diametral clearance and filled with heavy lubricating oil) as to cast serious doubts on the hysteresis results obtained, since the dashpot is necessarily in parallel with the specimen.

To overcome these difficulties a damping property would have to be introduced into the pneumatic unit itself, thus overcoming the inherent instability. It is worth pointing out at this stage that even if an elastic spring of the same stiffness were introduced in place of the pneumatic unit the system would still have a very small damping coefficient due primarily to the large effective mass of the pendulum.

3.53 Stabilized pneumatic load measuring unit.

After some consideration the scheme shown diagrammatically in Fig. 3.53 was adopted and, when properly adjusted, found to be completely successful. In this arrangement the fixed inlet choke of Fig 3.52 is replaced by a variable inlet jet similar to the main working jet. This inlet jet impinges on a plate forming the cap of a spring loaded bellows, subject to a differential pressure p - p'. Pressure p is the main jet pressure while p' is obtained by passing air via choke Q to the manometer which has an appreciable air capacity.

Now consider the conditions when the pendulum is moving towards the working jet. In the simple unit with a fixed inlet choke pressure p would be rising towards a value defined by the instantaneous jet gap. In the stabilized unit of Fig. 3.53 the fact that p is rising (due to the change in the working jet gap) causes a

downwards deflection of the bellows cap since because of the choke Q pressure p' will lag behind p. This opening of the inlet jet will increase pressure p. Conversely if the pendulum is moving away from the working jet pressure p will be falling and will suffer a further fall due to the closing of the inlet jet and thus by this device we can make pressure p dependent to some extent on the pendulum velocity. This effect if properly adjusted tends to damp out any oscillations that may occur.

It will be noticed that the actual load measurements are taken at pressure p' whereas the pendulum load is proportional to p. It is, however, important to reduce as far as possible the capacity of the main chamber at pressure p and since over a comparatively long term, say 1 minute, p' must equal p, pressure measurements are conveniently taken at p'. In additions the pressure readings should theoretically be independent of the main supply pressure. It is found in practice that there is a slight dependence on the supply pressure but this is easily counteracted by manual adjustment of a bleeder valve on the air supply line. The compressed air is supplied by a small vane type compressor (ex-R.A.F. vacuum pump) driven by a $\frac{1}{2}$ h.p. motor.

A mathematical analysis of the stability of these various pneumatic systems is given in Section 8 but due to the inherent non-linearity of the pneumatic effects these calculations can only be used as a design guide, a good deal of adjustment being necessary to attain successful operation.

Finally it should be noted that with this system of load and deflection measurement the pendulum is supported on the specimen alone and has no contact with any other part,

the only external force acting being the air pressure at the main jet. Consequently there is no possibility of mechanical friction effects influencing the final results.

3.6 Specimen clamping.

It is important that no slipping should occur at the clamping points of the specimen since this would appear in the final results as additional hysteresis. When the apparatus was first constructed the specimen and clamps used were as shown in Fig. 3.61. These were found ineffective in a rather fortuitous manner which is nevertheless worthy of putting on record. It was noticed that the loops obtained had an overall curvature as shown in Fig. 3.62. This could be due to some assymmetrical feature of the apparatus and an inspection it was noticed that both clamps were on one side of the specimen. When the specimen was redesigned with heavier ends and the much heavier clamps shown in Plate 3 fitted the curvature effects in the observed loops dissappeared. Since this observation it has been assumed that the efficiency of clamping can be judged from the symmetry of the observed loops.

3.7 Procedure for inserting specimen in apparatus.

The specimen must be inserted in the apparatus without the danger of being overstressed in the process. To attain this end a definite procedure has been evolved. This is as follows:-

(1) measure the actual breadth and thickness of the specimen at the minimum section,

(2) clamp the specimen firmly at its upper end to the central block of the horizontal arm, the pendulum bar having been removed,

(3) support the horizontal arm at each end by slip blocks resting on the upper frame-work of the apparatus. Adjust the slip blocks until the lower end of the

specimen is parallel to the clamping pillar as judged by feeler gauges.

(4) Keeping slip blocks in place very lightly clamp the lower end of the specimen - initially sliding the horizontal arm slightly to the right to bring the specimen into contact with the clamping pillar.

(5) Clamp the pendulum to central block of the horizontal arm and correct any deviation from vertical in the plane at right angles to the main bending plane. The purpose of the rather elaborate pendulum clamping mechanism (a cam rotated by a screw operated lever) is to avoid loading the specimen by heavy spanner forces when clamping the pendulum,

(6) firmly clamp the lower end of the specimen to the clamping pillar.

By these operations we arrive at a condition in which the specimen is fixed in the apparatus under zero or very little bending stress with the slip blocks still in place. This pendulum position can be taken as the datum for deflection measurements and hence the next step is

(7) fix datum for deflection measurements using the load measuring unit as a pneumatic gauge, i.e. still keeping slip blocks in position bring the working jet up to the pendulum until the manometer reading is approximately half of the supply pressure. Then without moving the micrometer screw slacken off and rotate the engraved micrometer head to give a convenient zero reading.

(8) insert the small stop nut of the load measuring unit - which prevents the pendulum from swinging out of range of the jet - and then remove the slip blocks which are no longer required.

(9) Correct any large static unbalance of the pendulum system by adjusting the levelling screws of the upper frame.

(10) Adjust the pendulum bob-weight to give the appropriate product Wy for the specimen being used. This adjustment is easily carried out by measuring the moment required to produce very small angular deflections of the system, the normal load and deflection measuring systems being used.

If required the load measuring unit is easily calibrated by keeping the micrometer screw fixed and observing the manometer readings when gram weights are added to a small scale pan suspended from the horizontal arm of the apparatus. This has been done on several occasions and all such calibrations have been linear and consistent with one another to within about 1% except at the extreme lower end of the manometer scale where some non-linearity is usually found. These calibration results also agree with the basic assumption that the force exerted by the working jet = jet pressure x jet area.

3.8 Influence of external disturbances.

Generally speaking sensitive apparatus is susceptible to external disturbance but due to the very low natural frequency of this equipment it is unaffected by normal floor vibrations. It is perhaps worth noting that the only other equipment known to the author based on the principle of off-setting a spring stiffness by an inverted pendulum is the Weichert Seismograph.

One type of disturbance to which this apparatus is, however, very susceptible is any minute tilt due to static deflection of the floor. Although the apparatus stands on a solid concrete floor manometer reading differences of 1 cm. can be obtained simply by walking from one end of the

equipment to the other, and it is therefore necessary to remain seated in one position while taking readings.

A similar effect, but of a more puzzling nature, occurred at one stage when it was found that the load readings crept upwards by about 20 cm. for about 2 hours after switching on the air compressor. This was traced to radiant heat from the compressor casing falling on one leg of the lower frame-work and producing a very small differential expansion.

4. Test results on mild steel.

4.1 Material and heat treatment.

Observations have been made of the non-linear properties of annealed mild steel at room temperature. No doubt many other experiments of interest could be made on other materials possibly at different temperatures but it was decided that for the purpose of a basic investigation observations should be confined to one material. Many hysteresis loops were plotted during the development of the apparatus, however, some for mild steel and others for a high carbon steel readily available in the workshop stores.

The main observations quoted in this section were made on mild steel during the summer of 1953. All specimens were cut from a single piece of 13/16" plate, tensile specimens 0.45" dia. and fatigue specimens for the Haigh machine 0.2" dia. being made at the same time. Prior to final machining all specimens were annealed by heating to 820°C. in an electric furnace and then allowing the closed furnace to cool overnight. A chemical analysis of the plate used gave the following principal constituents.

Carbon, 0.1% ; Manganese, 0.55% ; Phosphorus, 0.013% ;
Sulphur, 0.066% ; Silicon, 0.040% .

The damping tests are supplemented by a few observations made on

mild steel specimens during the final development of the apparatus in 1952. Unfortunately related tests - e.g. tensile, fatigue - were not made on this material so that from these particular observations only qualitative conclusions can be drawn.

4.2 Tensile tests.

Tensile tests were carried out on three annealed specimens and on one specimen in the as-rolled condition. The test results are given in Table I below.

TABLE I

Tensile Test Results.

Specimen	Young's Modulus E lb/in^2.	Limit of proportionality ton/in^2.	Yield Point ton/in^2.	Ultimate Strength ton/in^2.	Elongation at fracture on 4" gauge length
A1	-	-	14.2	22.2	33.6%
A2	30.5×10^6	13.6	15.1	23.7	31%
A3	-	-	13.1	22.2	32%
As rolled	-	-	14.5	25.6	Broke at gauge points

These results were obtained on the Buckton 10 ton capacity testing machine, a spring balance load measuring arrangement being used for two of the tests. The test procedures were briefly as follows:-

Specimens A1 and A3 Loaded with spring balance arrangement until extensions reached about 5% as measured with a dial gauge extensometer of 4" gauge length. Unloaded and extensometer removed. Reloaded immediately to fracture.

Specimen A2. Carefully loaded up to the yield point using the normal jockey balance, extensions being measured with a Lamb's roller extensometer. Unloaded after yielding and extensometer removed. Reloaded next day to give ultimate strength and elongation.

As rolled specimen. Loaded using jockey balance and yield point determined by dividers in gauge points. Loading continued to determine ultimate strength.

4.3 Fatigue Tests.

As it has often been suggested that there might be a correlation between damping capacity and fatigue endurance of materials a simple fatigue test was carried out on the material. This test was done in the Haigh machine using specimens of 0.2" minimum dia. The S - N curve obtained is given in Fig.4.3 the endurance limit for pure alternating stress being taken from this as ± 24000 lb/in^2.

4.4 Single loading linearity test.

The damping apparatus can be used to determine accurately the deviation from true linearity in the moment - angular deflection curve of the specimen and one speciment (D2) was tested in this way. The effect is illustrated in Fig.4.4.1 the truly elastic line being taken as the tangent to the actual moment - angular deflection curve at zero stress.

When analysing a test of this type it is desirable to take account of various small effects which may be neglected when observing simple hysteresis loops. Referring to Fig.4.4.2 where

M = actual internal moment in the specimen

m' = moment reading on pneumatic loading gauge,

Q = weights added to scale pan which are used to extend the range of the load measuring equipment

the equilibrium equation of the system is

$$M + 6.03\ Q \cos\theta + M' = Wy \sin\theta \quad \ldots\ldots\ldots\ldots 4.4/1$$

The appropriate value of Wy is found by weighing and balancing the pendulum and cross arm assembly after completion of the test, the result obtained in this case being 541 lb.in.

Taking the first two terms of the sine and cosine factors in equation 4.4/1 we obtain

$$M + 6.03\,Q\left(1 - \frac{\theta^2}{2}\right) + m' = 541\left[\theta - \frac{\theta^3}{6}\right]$$

The function $\underline{m}$ which we wish to determine is the difference between the actual resisting moment M and the truly linear moment $541\,\theta$,

$$\text{i.e.} \quad m = 541\,\theta - M$$

$$= m' + 6.03\,Q\left(1 - \frac{\theta^2}{2}\right) + 541\,\frac{\theta^3}{6} \quad \ldots\ldots 4.4/2$$

Working Units.

Unit angular deflection is taken as 0.01" at the micrometer screw which acts at $13\frac{3}{8}$ inches radius from the pivot of the swinging plate P.

Thus unit deflection $(\delta = 1) = \frac{0.01}{13.38} = 0.000748$ radians

$$\theta = 0.000748\,\delta \text{ radians.}$$

It is rather convenient that this unit deflection corresponds almost exactly to a bending stress in the specimen of 1000 lb/in^2. Unit moment $\underline{m}$ is taken as the moment producing 1 cm. rise on the load gauge manometer. By calibration this is 0.00296 lb.in. Scale pan load Q is provided by gram weights. 1 gram at this point gives a reading of 4.5 cm. on the load gauge manometer.

Substituting these values in equation 4.4/2 we find

$$m = m' + 4.5Q - 1.26 \times 10^{-6}\,Q\delta^2 + 12.8 \times 10^{-6}\,\delta^3 \quad \ldots\ldots 4.4/3.$$

The third term is this expression is found to be negligible. In addition we must take account of the initial values of m', $\left(\frac{\partial m'}{\partial \delta}\right)$ and Q, by the subtraction of the appropriate quantities which are $m'_0 = 21.0$, $\delta\left(\frac{\partial m'}{\partial \delta}\right)_0 = -0.3\delta$ and $Q_0 = 50$ in the particular test being analysed.

The final expression for moment m is therefore

$$m = (m' - 21.0) + 0.3\delta + 4.5(Q - 50) + 12.8 \times 10^{-6}\delta^3 \quad \ldots\ldots 4.4/4$$

this being the quantity plotted in Fig. 4.4.3. This

figure includes scales giving the approximate total moment M, maximum bending stress, and the deviation moment m in lb.in. The comparable test results obtained on mild steel specimens during 1952 are also shown in this figure.

In all cases it is seen that m rises steadily with deflection δ up to a certain value of M after which it increases much more rapidly.

At high stresses it was found that the value of m varies with the time from the application of the increment deflection. The nature of this time variation is shown in Fig. 4.4.4. For stresses just above the bend in the m v. M curve the "relaxation time" T is only a few minutes but this increases up to about half an hour for high stresses close to the yield point. The readings shown for specimens (1) 1952 and D2 - 1953 are those obtained immediately on loading. For specimen (2) the readings are those allowing for all creep effects to take place.

As the relaxation time T varies with the applied stress it is possible that the creep effects are present at all stresses, being short and masked by the operating time of the load measuring equipment at low stresses. It is clear, however, from a comparison of the curve for specimen (2) with those for specimens (1) and D2 that the time effect is much smaller than the main deviation effect: which apparently occurs instantaneously.

4.51 Damping tests for reversed stresses - Specimen D3.

This specimen was set up in the apparatus and subjected to the following stress programme in the order stated:-

Bending stress ± lb/in^2	No. of cycles.
4000	100
8000	100
12000	51
16000	10
20000	10
22000	10
25000	1

Measurements were taken of about 4 hysteresis loops, e.g. 1st, 2nd, 5th, 10th at each stress range. Time was not allowed for any creeping action to take place the individual loop points being observed at regular one minute intervals.

A typical plotted loop and the calculation of the corresponding damping capacity is given in Fig. 4.5.1 Table I summarizes all the results obtained on this specimen and those are illustrated in Figs. 4.5.3 and 4.5.4 Fig.4.5.4 also gives the damping results obtained on specimen D4 (see under). Fig.4.5.2 shows all the 5th cycle loops superimposed on one another assuming that all have the same mid-point.

From these numerical values it is seen that from the lowest stresses measured up to about ± 22000 lb/in^2. the damping coefficient rises from about 0.004 to 0.017. The loops in the upper part of this stress range (see Figs. 4.5.1 and 4.5.2) have a distinctive shape in that the main curvature occurs on the unloading part of the cycle. Variation of damping capacity with number of cycles of stress (see Fig. 4.5.3) is not present to any marked extent except at the highest stresses where some creeping action was also noted.

When the stress amplitude was increased to ± 25000 lb/in^2. a change in the whole nature of the hysteresis loop was noted the damping coefficient at this stress being about 80% greater than that at - 22000 lb/in^2. The loop shape showed a distinct curvature in the loading parts of the cycle and the increase in damping from the first to the second cycle was so great as to make observations of the second loop impossible.

4.52 Damping tests for reversed stress - Specimen D4

In the hope of obtaining more information on the nature of the hysteresis loop at high stresses this specimen was set up and tested in the stress range ± 18000 to ± 30,000 lb/in^2 only one or two cycles of stress being imposed at each stress level. The damping results obtained are plotted with those for specimen D3 in Fig. 4.5.4.

Although the damping values obtained are rather lower than those for D3 the damping coefficient - stress amplitude curve has the same general features. No marked curvature was, however, found on the loading portions of the higher stress cycles and only very slight creeping action was noticed at the highest stress ranges.

It may be observed at this point that many investigators have found large differences in the damping capacities of specimens nominally similar, although the results for each specimen are self-consistent.

5. Discussion of results.

5.1 Comparison with other investigators.

The results obtained agree, so far as they are directly comparable, with those obtained by other investigators.

Dorey's experiments in torsion on an 0.21% carbon steel having a tensile yield stress of 16 ton/in^2 gave values of the energy dissipation equivalent to a damping coefficient D of 0.023 for an alternating shear stress of ± 5.92 tons/in^2. Below this stress the energy dissipation varied approximately as the 2.8th power of the stress amplitude but a plot of the actual damping coefficients gives a curve very similar to that shown in Fig. 4.5.4 for specimen D3. Above the "critical stress" of ± 5.92 ton/in^2

Dorey found the damping coefficients to vary as about the 8th power of the stress amplitude. Thus the damping results obtained agree in magnitude and form with those obtained by Dorey on a similar material.

Lazan and Wu have carried out a series of tests on mild steel in alternating bending (Wohler test). They concluded that below a "cyclic stress sensitivity limit", which is rather less than the fatigue limit, damping capacity did not change with the number of cycles of applied stress. Between this "sensitivity limit" and the fatigue limit they found that the damping increased with the number of cycles of applied stress but not to any great extent in the first hundred cycles. These conclusions are consistent with the results obtained on specimen D3.

5.2 Before discussing the experimental results in detail some attention must be paid to the relationship between results obtained on a bending specimen, where the stress varies from point to point, and the more fundamental results which would be obtained on a uniformly stressed specimen.

It is shown in Section 6 that if a specimen in which the stress varies from 0 to F, has an overall damping coefficient D(F) then the damping coefficient d(F) of the same material subject to a uniform stress F is given by

$$d(F) = \sum_{n=0}^{\infty} a_n F^n \left(\frac{d^n D(F)}{d F^n} \right)$$

in which the coefficients a_n depend only on the stress distribution in the specimen.

A similar result is obtained in the analysis of the relationship betwen the stress deviation and the moment deviation on a single loading.

We can draw two general conclusions from the nature of the relationship stated above.

(1) Due to the importance of the derivatives of the observed function any sharp bends in the observed relationship between D(F) and F say, will be, if anything, accentuated in the derived results d(F). A well known inverse example of this effect is the smoothing of the yield curve in a bending test on a rectangular specimen.

(2) For the particular case in which the observed function can be expressed in the form F^K the derived function has the form bF^K where the coefficient b depends on the initial coefficients a_n and the value of the index K. Thus for this type of relationship the conversion from results obtained on non-uniformly stressed specimens to the equivalent uniform stress result is a conversion in magnitude only but not in form.

5.3 Discontinuity in experimental curves.

A prominent feature of the experimental results obtained for the deviation moment m, and the damping coefficient D, is the discontinuity occurring at high stresses - about 20,000 lb/in^2. Dorey noted a similar discontinuity occurring at a comparable stress. Apart from the change in the nature of the damping-stress curve, time effects in the deviation moment m results, and changes in damping with number of stress cycles, also became apparent at about this same stress.

It is probable that this discontinuity indicates a fundamental change in the damping process and it seems reasonable to discuss separately the results obtained above and below this "critical stress".

5.4 Results obtained above the critical stress.

The results obtained above the critical stress are distinguished from the others mainly by their magnitude and

rapid rise with increasing stress. This change in magnitude is such as to make the hysteresis loops and non-linearities measurable by a normal extensometer. Bairstow's experimental results appear to be confined to the stress range between the critical stress and the yield point. It is probable that the rise in the deviation moment curve above the critical stress corresponds to the curved part of the normal stress-strain relationship lying between the Limit of Proportionality and the Yield Point.

From the reasoning given later, (Section 5.52) it appears probable that hysteresis and other non-linear effects at these high stresses are caused by the yielding of small amounts of the material having a less than average yield strength.

5.51 Results obtained below the critical stress.

Considering the geometrical features of the hysteresis loops at stresses below the critical stress - Figs. 4.51 and 4.52 - and the corresponding curve of moment deviations for a single loading, Fig. 4.43 we find a complete lack of comparable information this being due primarily to experimental difficulties.

Bairstow's measurements of hysteresis looping at high stresses definitely show the main loop curvature in the loading section. Rowett's determination of the loop shape is based on the assumption that the loop is symmetrical about an elastic line and so cannot be regarded as conclusive. Many investigators have tacitly assumed that the loop is either evenly curved, or has its main curvature in the loading section, as can be seen from the explanatory diagrams in most papers.

Examining Fig. 4.5.2 we see that for low stresses the curvature of the loop does occur in the loading section.

As the stress amplitude increases the curvature moves back into the unloading section until at stresses just below the critical stress the loading portions of the loops are very accurately linear. It also appears that the slope of the loop curve - i.e. the instantaneous elastic modulus of the material - is the same at the start of the unloading portion for all stresses.

Considering the deviation moment curve - Fig. 4.4.3 - we see that up to the critical stress the results could be expressed approximately by an expression of the form $m = af^n$ with n rather less than 2. Double differentiation of this expression would give the curvature of the m versus f line and since $n < 2$ this would show high curvature at the lower stresses the curvature decreasing as the stress increased.

Some confirmation of these effects can be obtained from results obtained by other workers if we make some simplifying assumptions as to the form of the hysteresis loop. Referring to Fig. 5.51 assume that the loop shape is made up of curves of the form

$$\text{Stress } f = E\epsilon - K\epsilon^n$$

Then the energy dissipation per cycle and loop area A are given by

$$A = 2\left[\int_0^{\epsilon_m} f \, d\epsilon - \tfrac{1}{2}\epsilon_m f_m\right]$$

$$= 2\left[\tfrac{1}{2}E\epsilon_m^2 - \frac{K}{n+1}\epsilon_m^{n+1} - \tfrac{1}{2}E\epsilon_m^2 + \tfrac{1}{2}K\epsilon_m^{n+1}\right]$$

$$= \left(\frac{n-1}{n+1}\right)K\epsilon_m^{n+1}$$

implying that the energy dissipation should vary as Stress^{n+1} and the damping coefficient as Stress^{n-1}. Now it has been found that for moderate stress ranges the energy dissipation varies approximately as Stress^K where K is rather less than 3. Thomson[15] in his discussion of damping

coefficient v stress curves states "With relatively few exceptions the curves for stresses well below the elastic limit are concave to the stress axis. At higher stresses the curve is convex to the stress axis getting steeper and steeper as the stress rises..." This would indicate that in the above discussion n should be rather less than 2, which in turn implies by double differentiation that the main loop curvature is in the unloading sections.

This approximate relationship between the indice of the damping coefficient and the position of the main curvature of the loop can be confirmed by reference to the details of the experimental results obtained on specimen D3. At the lowest stresses the slope of the log D - log F curve is high and the loop curvature is in the loading position. As the stress amplitude rises $\left(\frac{d(\log D)}{d(\log F)}\right)$ falls and the loop curvature moves into the unloading sections. These actions are again reversed after the sharp upward bend in the log D - log F curve.

Since the difference betwen a linearly elastic material and one showing hysteresis looping and other non-linear effects lies in the curvature of the stress-strain relationship we conclude that the effects causing hysteresis etc. below the critical stress must occur primarily at comparitively low stresses.

5.52 Possible nature of the hysteresis effect.

If we assume that perfect metal would show true linear elasticity then the existence of non-linear effects such as hysteresis looping implies imperfection which could occur in one of several different ways. Various possibilities are -

(a) the metal is homogeneous but slight plastic flow occurs at all stresses however small,

(b) The metal is inhomogeneous containing a number of weak parts which yield at comparatively low stresses,

(c) the metal itself is of uniform strength but contains in its bulk small discontinuities which cause local plastic flow by reason of the stress concentration they produce.

In both of cases (a) and (b) we should expect the incremental plastic effect to increase with increasing stress.

Considering for example case (b)

Let g de = relative volume of material failing in the nominal elastic strain range ϵ to ϵ + de.

We should expect more material to fail between say 9 and 10 tons/in^2 stress than between 2 and 3 tons/in^2 stress, i.e. we should expect g to increase with stress. It is easily shown that the actual stress-strain curve of the material is given by $\int (\int g\ de)\ d\sigma$; - taking appropriate constants of integration - and thus g represents directly the curvature of the stress-strain relationship.

From the experimental observations it was concluded that the principle curvatures occurred at low stresses and since the curvature g is assumed for either cases (a) or (b) to increase with stress neither of these hypotheses agree with the experimental facts except at stresses above the critical stress.

An exact analytical investigation of case (c) would constitute a major mathematical problem but for a qualitative discussion we can assume that a small proportion of the material is subjected to a strain many times greater than the average. This condition is represented by the system of tie members shown in Fig. 5.52.1. If the application of load W causes an extension x then the strain

in member A will be $\frac{X}{L}$. The corresponding strain in member B will be confined mainly to the necked portion and will have a value $\doteqdot \frac{X}{e}$. It is easy to imagine a ratio $\frac{L}{e}$ such that when the composite member AB is loaded member A remains elastic and member B yields. If we deal with an alternating strains $\neq X_1$ and $\neq X_2$ the individual and composite load diagrams will be as shown in Figs. 5.52.3 and 5.52.4 respectively. These hysteresis loops have the same geometrical features as regards curvature - in this case a single bend - as the observed loops on specimen D3. Also for a single loading the load deflection diagram Fig. 5.52.2 shows a single change of slope at a comparitively low stress followed by a displaced elastic line.

5.53 Subsidiary tests on notched steel specimens.

To test the validity of this simple treatment of the elastic - plastic conditions near a point of high stress concentration careful tensile tests were made on notched specimens having the form shown in Fig. 5.53. These specimens were cut from the same plate as the others used in the main tests. Specimen 1 (unnotched) and Specimen 2 (notched as shown) were used to check the consistency of the material and the ultimate strength of the notched specimen respectively.

Specimen 3 was inserted in the 10 ton testing machine and a roller extensometer fitted over the 2" gauge length spanning the 3 notches. A load of 3000 lb. was then applied and removed in steps of 100 lb. extensometer readings being taken at each step. A further loading and unloading of 3000 lb. by steps of 500 lb. was then made. The observed load extension diagrams for the process are shown in Fig. 5.53 in which the non-linear effects have

been accentuated by subtracting from the extensometer readings a quantity accurately proportional to the applied load. This figure also gives the corresponding load - extension curves for specimen 4 which was subjected to repeated loadings of 2000, 2400, 2800 and 3200 lb.

These observed curves confirm the simple treatment given for the effects of stress concentration. The curve for the first loading of specimen 3 has a distinct bend at about 600 lb. load and is practically linear thereafter. The various hysteresis loops all show distinct curvature shortly after the start of loading or the start of unloading.

5.54 From those comparisons it appears probable that damping effects and other deviations from true linearity at stresses below the critical stress are due to the plastic flow at discontinuities in the bulk of the material. The existence of large numbers of discontinuities having various stress concentration factors would account for the smoothing of the angular loops caused by a single discontinuity into the forms of the corresponding experimental curves obtained on the damping specimens.

5.6 Conclusions.

From the test results and their comparison with those obtained by other investigators it is concluded that

1. The apparatus developed as part of this research gives reliable indications of the damping effects in mild steel specimens at moderate stresses. The sensitivity is better than has previously been attained in static tests.
2. When a specimen is subjected to a single static loading the resulting load-extension diagram shows a regular departure from the linearity right from the start of loading. This deviation varies approximately as stress f^n with n rather less than 2.

3. Hysteresis loops measured at low stress amplitudes show their main curvature in the loading parts of the stress cycle. As the stress amplitude increases the loop curvature moves back into the unloading part of the stress cycle, the loading parts becoming very straight. This is in contradiction to what has been tacitly assumed by many investigators, but agrees with conclusions which can be drawn from the accepted form of the relationship between damping coefficients and stress amplitudes.

4. These various effects are consistent with the assumption that damping and other non-linear properties are caused by plastic flow near discontinuities in the body of the material.

6. The calculation of the damping coefficient, or the stress deviation in a uniformly stressed part from the results of a test on a specimen in which the stress varies from point to point.

6.1 General. Due to convenience in loading and strain measurement, tests on materials are often carried out in bending or torsion or in some other manner in which the stress is not uniform throughout the specimen. If the quantity being observed, such as damping capacity, varies with stress then the experimental results represent an integral of the desired quantity throughout the specimen. It is important to devise an analysis whereby such readings may be converted to the more useful results which would be obtained on a uniformly stressed specimen, since otherwise the damping capacity of an arbitrarily shaped part can only be obtained from experiments on the part itself, or scale models of it.

Some forms of this analysis have been given by Föppl, Nadai (8), Thompson, and in the discussion of Dorey's paper. All these deal with the simple cases of a circular

rod in torsion or a rectangular section beam in uniform bending.

6.2 Analysis of damping coefficients.

Taking the damping coefficient as previously defined

let $D(F)$ = overall damping coefficient of the specimen when subjected to a maximum (as regards position in the specimen) alternating stress F.

$d(f)$ = damping coefficient of the metal when subjected to a uniform alternating stress f.

If the stress f at any point in the specimen is defined as a fraction ρ of the maximum stress F, i.e. $f = \rho F$, then the stress - volume distribution can be represented by a function v of ρ such that $v\,d\rho$ = volume of material in the stress range

$$\rho F \text{ to } (\rho + d\rho) F.$$

If furthermore we assume the hysteresis loops to be so small as to make practically no difference to the elastic modulus of the material - then

The maximum strain energy stored in the specimen $= \int_0^1 \frac{\rho^2 F^2}{2E} v\,d\rho = \frac{F^2}{2E}\int_0^1 \rho^2 v\,d\rho.$

and the total energy dissipated per cycle

$$= D(F)\,\frac{F^2}{2E}\int_0^1 \rho^2 v\,d\rho \qquad \text{.... Eqn (1)}$$

By integration the total energy dissipation per cycle is also

$$= \int_0^1 d(\rho F)\,\frac{\rho^2 F^2}{2E} v\,d\rho = \frac{F^2}{2E}\int_0^1 d(\rho F)\,\rho^2 v\,d\rho \qquad \text{.... Eqn (2)}$$

$$\therefore D(F)\int_0^1 \rho^2 v\,d\rho = \int_0^1 d(\rho F)\,\rho^2 v\,d\rho \qquad \text{.... Eqn (3)}$$

The right hand integral can be expanded as

$$\int_0^1 d(\rho F)\,\rho^2 v\,d\rho = \left[d(\rho F)\int \rho^2 v\,d\rho\right]_0^1 - \left[F\frac{\partial}{\partial(\rho F)}\{d(\rho F)\}\iint \rho^2 v\,d\rho\,d\rho\right]_0^1$$

$$+\left[F^2\frac{\partial^2}{\partial(\rho F)^2}\{d(\rho F)\}\iiint \rho^2 v\,d\rho\,d\rho\,d\rho\right]_0^1 \text{ — etc.}$$

$$= d(F)\int_0^1 \rho^2 v\,d\rho - F\frac{\partial}{\partial F}\{d(F)\}\int_0^1\int \rho^2 v\,d\rho\,d\rho \ldots$$

$$+ F^2\frac{\partial^2}{\partial F^2}\{d(F)\}\int_0^1\iint \rho^2 v\,d\rho\,d\rho\,d\rho \text{ ---etc. ..Eqn (4)}$$

And thus from equations (3) and (4)

$$D(F) = A_1\, d(F) - A_2\, F \frac{\partial}{\partial F}\{d(F)\} + A_3\, F^2 \frac{\partial^2}{\partial F^2}\{d(F)\} \ldots \text{ etc.}$$

..... Eqn.(5)

where $A_1 = \dfrac{\int_0^{\prime} \rho^2 v\, d\rho}{\int_0^{\prime} \rho^2 v\, d\rho} = 1$ $\quad A_2 = \dfrac{\int_0^{\prime}\int \rho^2 v\, d\rho\, d\rho}{\int_0^{\prime} \rho^2 v\, d\rho}$ $\quad A_3 = \ldots$etc.

From equation (5), D(F), and its successive differentials, with respect to F, can be expressed as

	d(F)	F d'(F)	F^2 d"(F)	
Coefficients	↓			
D(F) =	A_1	$-A_2$	A_3	..... etc.)
F D'(F) =	0	$(A_1 - A_2)$	$(-A_2 + 2A_3)$	..... etc.)
F^2D"(F) =	0	0	$(A_1 - 2A_2 + 2A_3)$	.... etc.)

..... Eqn. (6)

where primes indicate differentiation with respect to F.

From these equations (6) d(F) can be determined by forming a linear function

$$d(F) = B_1\, D(F) + B_2 F\, D'(F) + B_3\, F^2\, d''(F) \ldots \text{ etc. } \ldots \text{ Eqn(7)}$$

the coefficients B being chosen so as to eliminate the derivatives of d(F). For this conditions the B's are given by

$$B_1 = \frac{1}{A_1} = 1$$

$$B_2 = \left(\frac{A_2}{A_1 - A_2}\right) B_1$$

$$B_3 = \frac{(-A_3)\, B_1 + (A_2 - 2A_3)\, B_2}{(A_1 - 2A_2 + 2A_3)}$$

etc.

The values of B_1, B_2 and B_3 for several specimen shapes of special interest have been calculated and are as follows:-

Specimen	$v = f(\rho)$	B_1	B_2	B_3
Uniform stress:- Direct tension or thin tube in uniform torsion	zero up to ρ close to 1.	1	0	0
Specimen used in this series of tests	Expressed graphically	1	+0.795	+0.406
Rectangular bar-uniform bending	Const.	1	$+\frac{1}{3}$	0
Solid circular section - uniform torque	Const. x ρ	1	$+\frac{1}{4}$	0
✱ Bar vibrating in fundamental longitudinal mode or thin tube in uniform bending	$\frac{1}{\sqrt{(1-\rho^2)}}$	1	+0.177	-0.01
✱ Solid circular section in uniform bending.	$\sqrt{(1-\rho^2)}$	1	+0.463	+0.032

✱ N.B. If the damping test is carried out by the method of lateral deflection in the Wohler test then these cases correspond to uniform stress and v = const x ρ respectively and the corresponding coefficients should be used.

It will be noticed that the derivatives of the observed function are of some importance in the final result and hence the above analysis is most useful when the experimental results can be expressed in some simple form. For the particular case in which

$$D(F) = a F^n$$

$$d(F) = B_1 a F^n + B_2 F a n F^{n-1} + B_3 F^2 a n(n-1) F^{n-2} \text{ etc.}$$

$$= a F^n \left[B_1 + n B_2 + n (n-1) B_3 \right]$$

i.e. $d(F)$ = constant x $D(F)$ where the constant is determined by the shape of the specimen and the observed value of index n .

6.3 Analysis of small amounts of plastic deformation in a specimen subjected to a uniform bending moment but of varying cross-section.

This analysis which may be used to obtain the stress deviation $\phi(s)$ in a uniformly stressed specimen from the moment deviation $\underline{m}$ observed on a bending specimen (see Fig. 6.3) is rather more difficult than the damping analysis given in Section 6.2. We cannot predict from the start the curve into which the specimen will bend and hence it is only possible to deal with cases in which the departure from true linearity - the plastic strain or the stress deviation - is small compared with the total strain or total stress. (This remark does not of course apply to the case of a beam with a uniform cross-section). The main case of interest is that of the specimens used in the present series of tests which are of rectangular cross-section of uniform width $\underline{b}$, and depth $\underline{d}$ varying along their length.
Let f = stress and s = strain and let $f = Es + \phi(s)$ where E = Young's modulus (See Fig. 6.3(a)). Taking a rectangular section b x d subject to a maximum strain S and assuming $\phi(s)$ to be a symmetrical function the total moment M (Fig. 6.3b) is given by

$$M = 2\int_0^{d/2} f\, b\, y\, dy = \frac{bd^2}{2S^2}\int_0^S f\, s\, ds$$

$$= \frac{bd^2}{2S^2}\int_0^S \left[Es + \phi(s)\right] s\, ds$$

$$= \frac{bd^2}{6} E S + \frac{bd^2}{2S^2}\int_0^S s\,\phi(s)\, ds$$

$$\therefore S = \frac{6M}{bd^2E} - \frac{3}{ES^2}\int_0^S s\,\phi(s)\, ds.$$

If as assumed $\phi(s) \ll Es$ then the value of S for the integral term may be taken as $\frac{6M}{bd^2E}$ and this gives

$$S = K\alpha - \frac{3}{EK^2\alpha^2} \int_0^{K\alpha} s\,\phi(s)\,ds \quad \ldots\ldots\ldots \text{Eqn (8)}$$

where $K = \frac{6M}{bE}$ which is constant along the specimen and

$\alpha = \frac{1}{d^2}$ which varies along the specimen.

If now the integral term is expanded by parts as in Section 6.2

$$s = K\alpha - \frac{3}{EK^2\alpha^2}\left[\phi(s)\int sds - \phi'(s)\iint sdsds + \phi''(s)\iiint s\,ds\,ds\,ds \text{ etc}\right]_0^{K\alpha}$$

$$= K\alpha - \frac{3}{E}\left[\frac{1}{2}\phi(K\alpha) - \frac{K\alpha}{6}\phi'(K\alpha) + \frac{K^2\alpha^2}{24}\phi''(K\alpha) \ldots \text{etc.}\right.$$

$$\ldots\ldots \text{Eqn (9)}$$

Now replace $\phi(K\alpha)$, $\phi'(K\alpha)$ etc by the appropriate Maclaurin series

i.e. $\phi(K\alpha) = \phi(K\alpha_0) + (K\alpha - K\alpha_0)\,\phi'(K\alpha_0) + \frac{(K\alpha - K\alpha_0)^2}{2}\phi''(K\alpha_0)$

$\ldots\ldots$ etc.

$\phi'(K\alpha) = \phi'(K\alpha_0) + (K\alpha - K\alpha_0)\,\phi''(K\alpha_0) \ldots\ldots$

$\phi''(K\alpha) = \phi''(K\alpha_0) \ldots\ldots$

and substituting this in equation (9) we obtain

$$S = K\alpha - \frac{3}{E}\left[\frac{1}{2}\phi(K\alpha_0) + K\left(\frac{\alpha}{3} - \frac{\alpha_0}{2}\right)\phi'(K\alpha_0)\right.$$

$$\left. + K^2\left(\frac{\alpha^2}{8} - \frac{\alpha\alpha_0}{3} \quad \frac{\alpha_0^2}{4}\right)\phi''(K\alpha_0) \ldots \text{etc}\right. \quad \ldots \text{Eqn (10)}$$

If θ represents angular deflection and x distance along the specimen then

$$\frac{d\theta}{dx} = \frac{2S}{d}$$

$\therefore\ \theta = \int \frac{2S}{d}\,dx$ and substituting for S from equation 10

we obtain

$$\theta = 2K\int \frac{\alpha}{d}\,dx - \frac{3}{E}\phi(K\alpha_0)\int \frac{1}{d}\,dx - \frac{6K}{E}\phi'(K\alpha_0)\int \left(\frac{\alpha}{3d} - \frac{\alpha_0}{2d}\right) dx$$

$$- \frac{6K^2}{E}\phi''(K\alpha_0)\int \left(\frac{\alpha^2}{8d} - \frac{\alpha\alpha_0}{3d} + \frac{\alpha_0^2}{4d}\right) dx \quad \ldots\ldots \text{ etc.}$$

The values of these integrals have been obtained graphically and by calculation for the specimen taking α_0 at the minimum section, and are 2320, 19.0, -1164 and + 82000 respectively. Thus

$$\theta = 4640\,K - \frac{57}{E}\phi(K\alpha_0) + \frac{7000K}{E}\phi'(K\alpha_0) - \frac{492000}{E}K^2\phi''(K\alpha_0) -$$

-- etc. ...Eqn. (11)

Inverting this equation by a similar process to that used between equations (5) and (7) Section 6.2 and also substituting the actual moment $M = \frac{bEK}{6}$ we obtain

$$\phi(K\alpha_0) = \phi \text{ (maximum strain)}$$

$$= 2462M - 526000\left[\theta + 1.53M\,\frac{\partial\theta}{\partial M} + 0.38M^2\,\frac{\partial^2\theta}{\partial M^2} \ldots \text{ etc.}\right]$$

.... Eqn. 12

It is now necessary to consider the relationship if this equation to the observed quantities. Referring to Fig. 6.3 and assume for the time being that the conditions are purely elastic i.e. $\phi(s) = m = 0$, $M = k\theta$ and $\frac{d\theta}{dM} = \frac{1}{k}$.
Substituting these values in equation (12) we can obtain the nominal elastic stiffness of the specimen

i.e. $0 = 2462M - 526000\left[\theta + 1.53\,k\theta.\,\frac{1}{k}\right]$

$$= 2462M - 2.53 \times 526000\,\theta.$$

$$\therefore M = \frac{2.53 \times 526000}{2462}\theta = \underline{541\,\theta}$$

$\therefore$ Angular stiffness = 541 lb.in./rad.

This value checks exactly with that obtained by a simple graphical calculation, and also with the experimental results.

Equation (12) gives ϕ (maximum strain) in terms of the plot if θ v M. It is more convenient to obtain $\phi(s)$ in terms

of the m v θ relationship. First eliminate the large linear part of equation (12) by the substitution

$$\theta = \frac{M}{541} - \gamma$$ $-\gamma$ being defined in Fig. 6.3.

This gives

$$\phi(s_{max}) = 526000\left[\gamma + 1.53\, M \frac{\partial \gamma}{\partial M} + 0.38 M^2 \frac{\partial^2 \gamma}{\partial M^2} \ldots \text{etc.}\right]$$

On further substitution of $M = 541\theta$ and $m = 541\gamma$ we finally obtain

$$\phi(s_{max}) = 973\left[m + 1.53\theta \frac{\partial m}{\partial \theta} + 0.38\theta^2 \frac{\partial^2 m}{\partial \theta^2} \ldots\ldots\right]$$

and this gives the stress deviation for a uniformly stressed specimen in terms of the moment deviation in a bending test. It will be noticed that if m = constant x θ^n then the above relationship can be expressed in the form

$$\phi(s_{max}) = \text{constant} \times m$$

where the constant depends on the value of the index n.

7. Methods of load and strain measurement tried during development of apparatus.

7.1 Oneof the major difficulties in the development of the apparatus described was the satisfactory measurement of the external moment acting in the pendulum. Several different systems of load and deflection measurement were tried before the satisfactory pneumatic system was devised and it may be of some value to place on record a brief description of these methods and why they were in fact unsatisfactory.

7.2 The first method tried was to place loading weights in a scale pan while a ball fixed to the horizontal loading arm of the machine rested between a pair of stops mounted on a small screw jack as shown in Fig. 7.2. It was intended to observe the deflection due to a given load by operating the screw jack until the ball just floated between the stops this condition being indicated by a simple system of electrical

contacts. This scheme was found very tedious to operate due to a slow bumping of the whole system between the stops, although this fault was somewhat alleviated by arranging a slow steady motor drive to the micrometer screw.

The serious fault mentioned on page 13 i.e. the impossibility of attaining a balance under certain conditions was however apparent and it was decided that the load system must be such that in practice the deflection θ should first be fixed and the required loading moment m should then be determined by some form of spring balance.

7.3 Following the reasoning given above a simple spring system was devised with optical measurement of load and deflection. Referring to Fig. 7.31 deflection of the pendulum and specimen is carried out by rotation of a threaded rod interposed between a cantilever spring and the end of the horizontal arm of the apparatus. Mirrors M_1 and M_2 mounted on the spring and arm respectively give an optical indication of load and deflection.

Readings were fairly easily obtained by this scheme but during operation rather violent oscillation of the whole system occurred and this was only slowly damped out. As a result of this two successive readings A and B (see Fig. 7.32) would not be the result of following the direct pattern AB but rather the result of following out the superimposed set of loops shown, and this would cast doubt on any readings obtained by this method.

7.4 The difficulty mentioned ~~in~~ above (~~b~~) could be overcome by greatly increasing the stiffness of the measuring spring and various methods were considered whereby a reliable indication of a small deflection ± say 0.001" - could be obtained.

After rejecting the possibility of mechanical or mechanical - optical systems - on the grounds of possible friction which would be of the same order as the load being

measured, - the electronic device shown in Fig. 7.4 was constructed. Here deflection of the spring S causes a change in the capacitance of C_1. This condenser along with a variable condenser C_2, is connected in the tuned circuit of a radio frequency oscillator and the output frequency is very accurately matched with that from a stable crystal oscillator. Thus the rotation of C_2 can be calibrated against the load exerted at the straining screw and measurements obtained by what is basically a null method. The circuit was first tried with a large pick-up unit capable of measuring loads up to about 20 lb. and was found to be accurate and reliable.

When, however, it was assembled with an appropriate pick-up in the main apparatus it was found impossible to obtain steady readings in the meter M. At the time this was ascribed to some undetermined fault in the rather complex electronic circuit - condenser C_1 with its now very small gap being particularly suspect. It is now clear that the real fault lay in the combination of the very stiff spring with the massive pendulum system. This whole arrangement would have a very small damping coefficient and thus oscillation of the mechanical system, due to manipulation of the straining screw would take a very long time to die out. This would prevent any effective null measurement of load. In addition it is now known that time effects can arise in the real measured load on the specimen and this would also impede the taking of null measurements.

7.5 Two systems in which operation is by setting a deflection and then slowly varying an applied load until balance is attained.

In the first of these systems (Fig. 7.5) the micrometer deflection screw is mounted on an arm attached to the shaft of a small (75 watts) motor. Balance is attained by passing a

current through the armature (the brushes having been removed and fine wires soldered to the appropriate commutator segments). With a fixed field current and a small armature current the armature torque is proportional to the armature current. The current is varied by a series resistance and measured by a milliammeter. The condition of balance is indicated by a simple system of stops and electrical contacts.

In the second of these two systems, tried after unsatisfactory results with the first, the use of the motor as a load measuring device was dispensed with. Instead, using the motor only as a bearing a piece of 1/8" dia. brass wire about 2 feet long was suspended from the motor arm near the stops (see also Fig. 7.5). This wire was inside a burette and by varying the level of water in the burette a suitable range of load on the motor arm could be obtained.

Both of these systems showed the same faults as the system described in Section 7.4 i.e. it proved impossible to obtain steady null readings. At this stage the conclusions given at the end in Section 7.4 were formed and in view of this it was decided to develop some form of automatic balancing system. This led to the pneumatic systems described in Section 3.5 of the main text.

8.1 The Stability of the pneumatic load measuring devices.

The pneumatic load measuring device used is only practicable when properly designed to give stable operation. The Leonhard stability criterion has been used in this design and may be briefly stated as follows. Suppose the differential equation controlling a response z is of the form $(D^n + aD^{n-1} + bD^{n-2} \ldots\ldots K)\, z = 0$. Now replace the differential operator D by the factor iw, $(i = \sqrt{-1})$, and

the function in brackets

$$(i\,w)^n + a\,(i\,w)^{n-1} \ldots\ldots\ldots K$$

will define a locus if w is treated as a variable (see Fig. 8.1). This locus will rotate through an angle $\frac{n\pi}{2}$ between $w = 0$ and $w = \infty$, and forms the Leonhard stability diagram. It is known that the solutions of the original equation are all stable (i.e. negative exponentials or decaying sinusoidal) provided that this locus encircles the origin of the diagram.

8.2 Simple pneumatic system.

Referring to Fig. 8.21, assume that the outlet flow rate is proportional to the outlet area and the square root of the pressure difference. For the conditions of small disturbance p and x shown.

Outlet flow rate

$$V + v = \text{constant} \times (X + x)\sqrt{\left(\frac{P}{2} + p\right)}$$

$$\doteq L\,(X + x)\left[\sqrt{\frac{P}{2}} + \frac{p}{2\sqrt{\frac{P}{2}}}\right]$$

$$= L\,(X + x)\left[s + \frac{p}{2s}\right]$$

where $s = \sqrt{\frac{P}{2}}$ and $p \ll \frac{P}{2}$

Under normal conditions

$$V = L\,X\,s$$

$\therefore$ Additional outlet flow $v = L\left[\frac{Xp}{2s} + xs\right]$ ignoring the product term in p x.

The normal inlet flow rate is $\frac{P - \frac{P}{2}}{R} = \frac{P}{2R}$ and the variation on this due to the disturbance p will be $-\frac{p}{R}$

$\therefore$ Total incremental inflow to the chamber (of capacity C) due to the disturbances p and x will be

$$C\frac{dp}{dt} = -\frac{p}{R} - L\left(\frac{Xp}{2s} + Xs\right)$$

$$= -p\left[\frac{1}{R} + \frac{LX}{2s}\right] - L\,s\,x$$

$$\therefore\ x = \frac{1}{Ls}\left[-C\frac{dp}{dt} - \left(\frac{1}{R}\ \frac{LX}{2s}\right)p\right]$$

In addition $M\frac{d^2x}{dt^2} = ap$

$$\therefore\ \frac{ap}{M} = \frac{1}{Ls}\left[-C\frac{d^3p}{dt^3} - \left(\frac{1}{R}\ \frac{LX}{2s}\right)\frac{d^2p}{dt^2}\right]$$

Converting this to the operational form and substituting iw for the differential operator D we obtain

$$-iw^3 - \frac{1}{C}\left(\frac{1}{R} + \frac{LX}{2s}\right)w^2 + \frac{a\,L\,s}{CM}$$

as the locus of the Leonhard diagram. This takes the form shown in Fig. 8.22 and as the diagram lies wholly below the real axis this system cannot possibly give stable operation.

8.3 Same pneumatic systems but with viscous damping of the pendulum:-

As in Section 8.2 the pneumatic equations lead to

$$x = \frac{1}{Ls}\left[-C\frac{dp}{dt} - \left(\frac{1}{R} + \frac{LX}{2s}\right)p\right]$$

but for the motion of the pendulum we have

$$ap = M\frac{d^2x}{dt^2} + b\frac{dx}{dt}$$

Using a process similar to that in Section 8.2 we obtain as the equation of the Leonhard stability locus.

$$iw\left[\frac{b}{MC}\left(\frac{1}{R} + \frac{LX}{2s}\right) - w^2\right] + \left[\frac{aLs}{CM} - w^2\left(\frac{1}{C}\left\{\frac{1}{R} + \frac{LX}{2s}\right\} + \frac{b}{M}\right)\right.$$

This will cross the imaginary axis at

$$w_n^2 = \frac{\frac{a\,L\,s}{CM}}{\frac{1}{C}\left\{\frac{1}{R} + \frac{LX}{2s}\right\} + \frac{b}{M}}$$

If the diagram is to encircle the origin then the coefficient of iw must be positive at this value of w^2

$$\therefore \text{For stability } \frac{b}{MC}\left(\frac{1}{R}+\frac{LX}{2s}\right) \geqslant \frac{\frac{a\,L\,s}{CM}}{\frac{1}{C}\left\{\frac{1}{R}+\frac{LX}{2s}\right\}+\frac{b}{M}}$$

Since all the quantities concerned are necessarily positive this condition will be satisfied if

$$b \geqslant \frac{a\,L\,s}{\frac{1}{C}\left\{\frac{1}{R}+\frac{LX}{2s}\right\}^2}$$

and this gives the required strength b of the viscous dashpot.

8.4 Final pneumatic unit:-

In the final design, viscous damping having been found impracticable, the damping process was introduced into the pneumatic unit as described in Section 3.53. The equations of this system (see Fig. 8.4) are rather more complex being of the fourth order instead of the third as were the previous sets. Referring to Fig. 8.4 in which the inlet and outlet jets are similar and the steady state conditions are given in capitals and the disturbances in the lower case letters.

Flow into the main chamber of capacity C_1.

$$= L\,(X+y)\left(s-\frac{p_1}{2s}\right) - L\,(X+x)\left(s+\frac{p_1}{2s}\right) - \frac{p_1-p_2}{Q} - A\frac{dy}{dt}$$

where L and s have the same significance as in Section 8.2.

Ignoring the products yp_1 and xp_1 we obtain

$$C_1\frac{dp_1}{dt} = Ls\,(y-x) - \frac{LXp_1}{s} - \frac{p_1-p_2}{Q} - A\frac{dy}{dt} \quad \ldots\ldots(1)$$

The relationships between p_1 and the other quantities are

$$M\frac{d^2x}{dt^2} = a\,p_1 \quad \therefore \quad \frac{d^2x}{dt^2} = \frac{a}{M}p_1 \quad \ldots\ldots\ldots\ldots(2)$$

Ignoring the relatively small effect of the bellows movement on pressure p_2

$$C_2 \frac{d\,p_2}{dt} = \frac{p_1 - p_2}{Q} \qquad \therefore\ p_1 - p_2 = Q\,C_2 \frac{dp_2}{dt} \quad .....(3)$$

$$p_1 = Q\,C_2 \frac{d\,p_2}{dt} + p_2 \quad .....(4)$$

$$y = \alpha\,(p_1 - p_2) = \qquad = \alpha\,Q\,C_2 \frac{d\,p_2}{dt} \quad .....(5)$$

By manipulation of Equations (1) to (5) we can eliminate all the variables other than p_2 and the final operational equation is

$$\left\{\left(D + \frac{1}{QC_2}\right)\left[D^3 + \frac{LX}{sC_1} D^2 + \frac{Lsa}{C_1 M}\right] + \left(\frac{1}{QC_1} - \frac{Ls\alpha}{C_1}\right) D^3 + \frac{A\alpha}{C_1} D^4\right\} (p_2) = 0 \quad .....(6)$$

and to facilitate the interpretation of this function let it be represented by

$$\{(\phi_1)\,[\phi_2] + (\phi_3) + \phi_4\}\ (p_2) = 0$$

Considering these terms one by one take first of all function ϕ_2. By inspection this corresponds exactly to the full stability function for the simple pneumatic system of Section 8.2. L, X, s, C_1, M and a are all determined by the "static" design of the unit, i.e. main jets and pendulum mass, and thus for any general layout function ϕ_2 is fixed. Function ϕ_1 represents the extra lag introduced to the system by the choke Q leading to the bellows and manometer, while ϕ_4 is the extra capacity introduced to C_1 by the action of the spring bellows.

Inspection of these functions when wi is substituted for D (see Fig. 8.4) shows that ϕ_3 gives only a vertical displacement to points on the stability locus. Now if the final locus is to encircle the origin it must cross and recross the imaginary axis and whether or not this occurs in determinable from the real parts of the function $(\phi_1)[\phi_2] + \phi_4$.

On substitution these are

$$\left(1 + \frac{A\alpha}{C_1}\right) w^4 - \frac{L\,X}{Q\,s\,C_1 C_2}\, w^2 + \frac{L\,s\,a}{Q\,M\,C_1\,C_2}$$

If we treat this as an equation for determining the values of w_n^2 at which the locus crosses the imaginary axis then it must have real solutions and hence as a first condition for stability

$$\left(\frac{L\,X}{Q\,s\,C_1\,C_2}\right)^2 > 4\left(1 + \frac{A\alpha}{C_1}\right)\frac{L\,s\,a}{Q\,M\,C_1\,C_2}$$

$$\therefore\ \frac{1}{QC_2} > 4\left(1 + \frac{A\alpha}{C_1}\right)\frac{s^3\,a\,C_1}{M\,L\,X^2} \qquad \ldots\ldots\ldots\ldots(7)$$

and this places an upper limit on the values of QC_2 and $A\alpha$. It will be noticed on purely physical reasoning that if the bellows and choke Q were fitted without their subsequent action on the inlet valve they would tend to have an unstabilizing effect on the system since they would increase the initial time lag. These primary considerations ensure that the locus diagram will cross the imaginary axis the relevant values of w^2 being

$$w_n^2 = w_1^2 \pm \varepsilon$$

where
$$w_1^2 = \frac{L\,X}{2\,s\,Q\,C_1\,C_2\left(1 + \frac{A\alpha}{C_1}\right)}$$

and
$$\varepsilon = \frac{\sqrt{\left[\frac{L\,X}{QsC_1\,C_2}\right]^2 - 4\left(1 + \frac{A\alpha}{C_1}\right)\frac{L\,s\,a}{QM\,C_1C_2}}}{2\left(1 + \frac{A\alpha}{C_1}\right)} \qquad \ldots\ldots(8)$$

Complete stability of the system will be ensured if in addition the locus intersects the real axis at some point to the left of the origin. Consideration of the imaginary parts of equation 6 (with iw substituted for D) shows that this intersection occurs at

$$w_r^2 = \frac{\frac{L\,s\,a}{C_1 M}}{\frac{1}{QC_2} + \frac{LX}{sC_1} + \frac{1}{QC_1} - \frac{L\,s\,\alpha}{C_1}} \qquad \ldots\ldots(9)$$

and hence the final stability condition is obtained by noting from the diagram that this value of w_r^2 must lie between the two values of w_n^2

$$\text{i.e. } w_1^2 - \varepsilon < w_r^2 < w_1^2 + \varepsilon \qquad \ldots\ldots(10)$$

Acknowledgements.

The work covered by this thesis was commenced under the supervision of the late Professor Gilbert Cook whose encouragement the candidate takes this opportunity of acknowledging. His thanks are due also to Professor James Small and the University of Glasgow for the facilities freely placed at his disposal.

BIBLIOGRAPHY

1. W. Thomson (Lord Kelvin) - On the Elasticity and Viscosity of Metals. - Proceedings of the Royal Society - Vol. 14 - 1865.

2. L. Bairstow - Elastic Limits of Iron and Steel under Cyclical Variations of Stress - Phil. Transactions of the Royal Society - Vol. 210.A. - 1910.

3. F. E. Rowett - Elastic Hysteresis in Steel - Proceedings of the Royal Society - Vol. A89 - 1914.

4. W. Mason - The Mechanics of the Wohler Rotating Bar Fatigue Test - Aeronautic Research Committee - R and M No. 838 - 1922.

5. H. J. Gough - The Fatigue of Metals - Scott, Greenwoods and Son - London, 1924.

6. O. Föppl, E. Becher, and G.S. von Heydekampf - Die Dauerprufung der Werkstoffe - Springer - Berlin, 1929.

7. G.S. von Heydekampf - Damping Capacity of Materials - Proceedings of the Amer. Soc. for Testing Materials - Vol. 31 - 1931.

8. A Nadai - Plasticity - McGraw-Hill Book Co. - New York, 1931.

9. S. F. Dorey. - Elastic Hysteresis in Crankshaft Steels. - Proceedings of the Institution of Mechanical Engineers - Vol. 123 - 1932.

10. W. Saran. - A Machine for Determining the Fatigue Limit of Metals. - Engineering - Vol. 133 - 1932.

11. O. Föppl. - The Practical Importance of the Damping Capacity of Metals especially Steels - Journal of the Iron and Steel Institute - Vol. 134 - 1936.

12. Anon. - Torsional Damping Recorder - Engineering - Vol. 144 - 1937.

13. E. Orowan. - Theory of Fatigue - Proceedings of the Royal Society. - Vol. 171.A - 1939.

14. W.H. Hatfield, G. Stanfield, and L. Rotherham. - The Damping Capacity of Engineering Materials - Transactions of the North-East Coast Institution of Engineers and Shipbuilders - Vol. 58 - 1942.

15. F.C. Thompson - Damping Capacity - Research Report of the British Non-Ferrous Metals Association - No. 657 - 1944.

16. C. Zener - Elasticity and Anelasticity of Metals - University of Chicago Press - 1948.

17. E. Linacre. - Damping Capacity - Iron and Steel. - Vol. 23 - 1950.

18. B.J. Lazan and T. Wu. - Damping, Fatigue and Dynamic Stress-Strain of Steel - Proceedings of the Amer. Society for Testing Materials. - Vol. 51 - 1951.

19. D. Morrison - Deviations from Hookes Law within the Elastic Range. Engineering - Vol. 177 - 1954.

LIST OF ILLUSTRATIONS

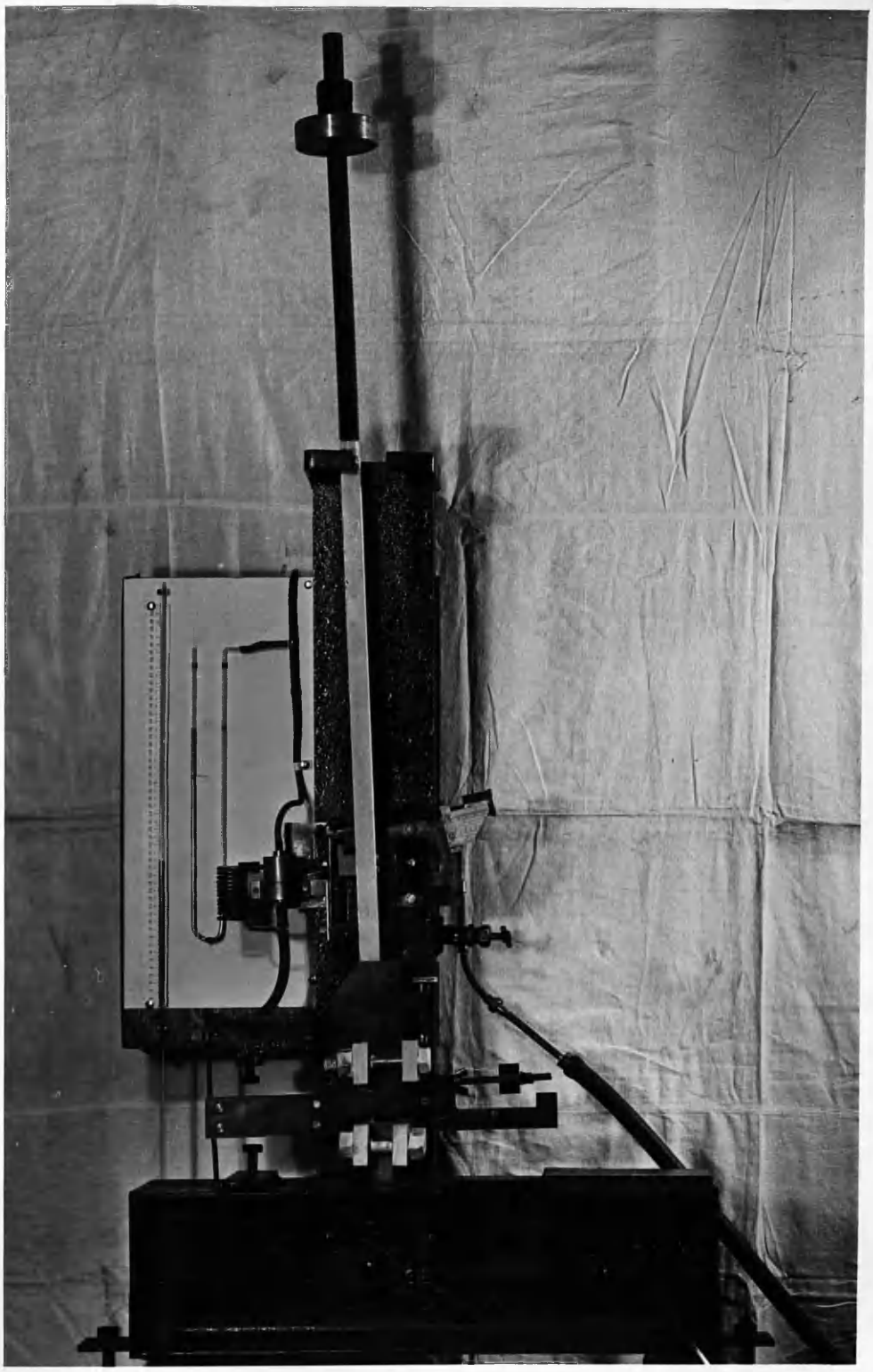

PLATE I.

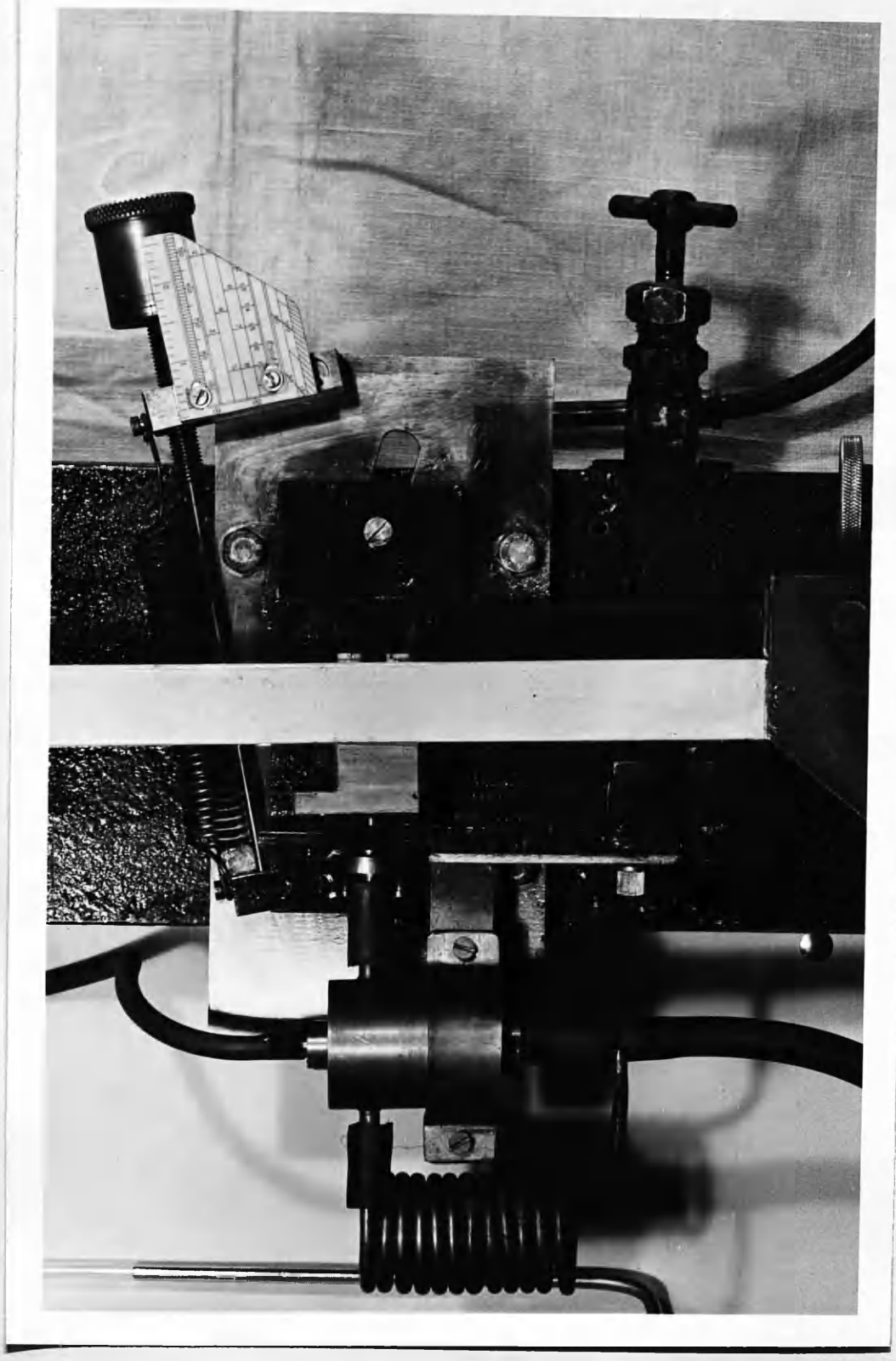

PLATE 2.

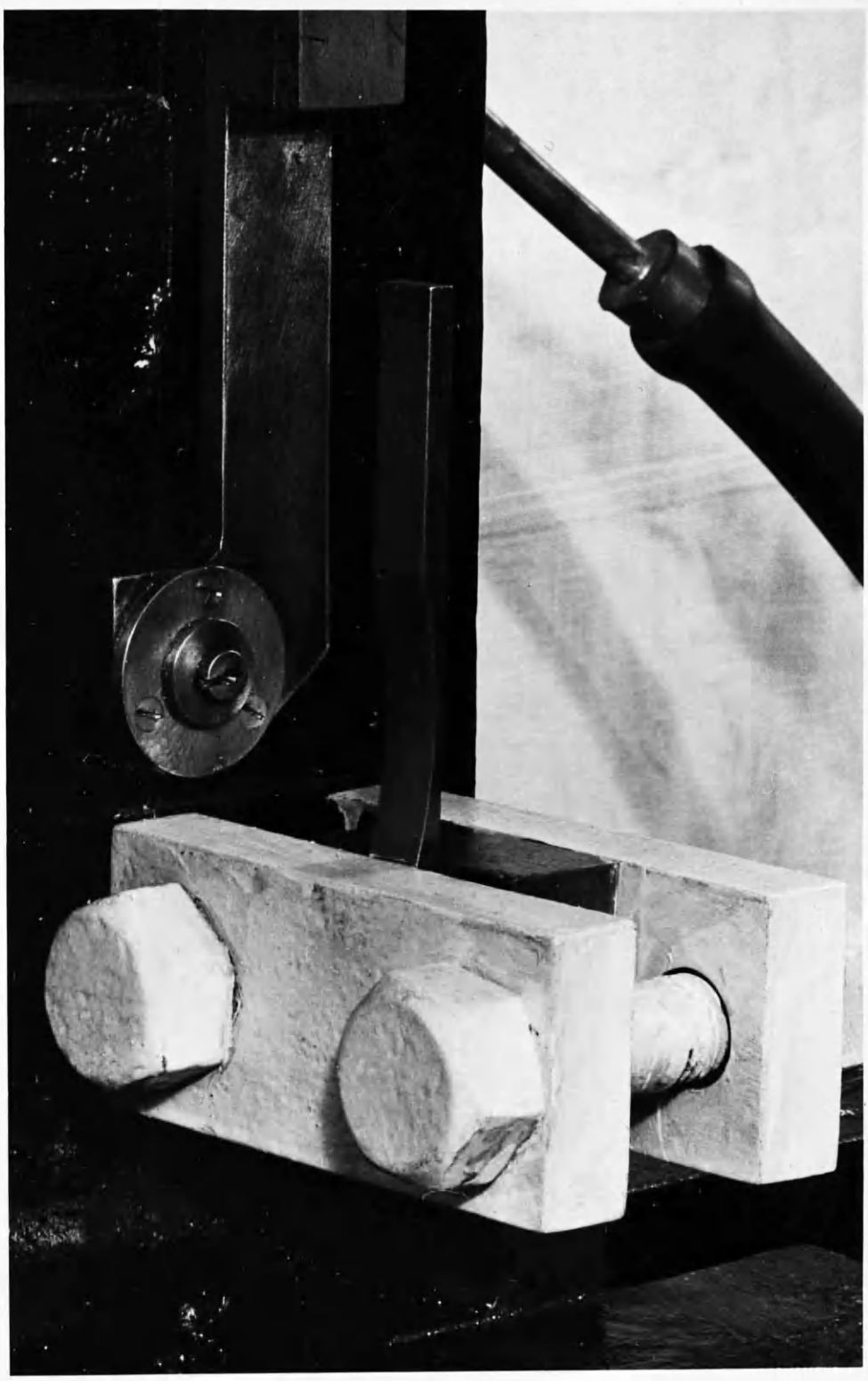

PLATE 3.

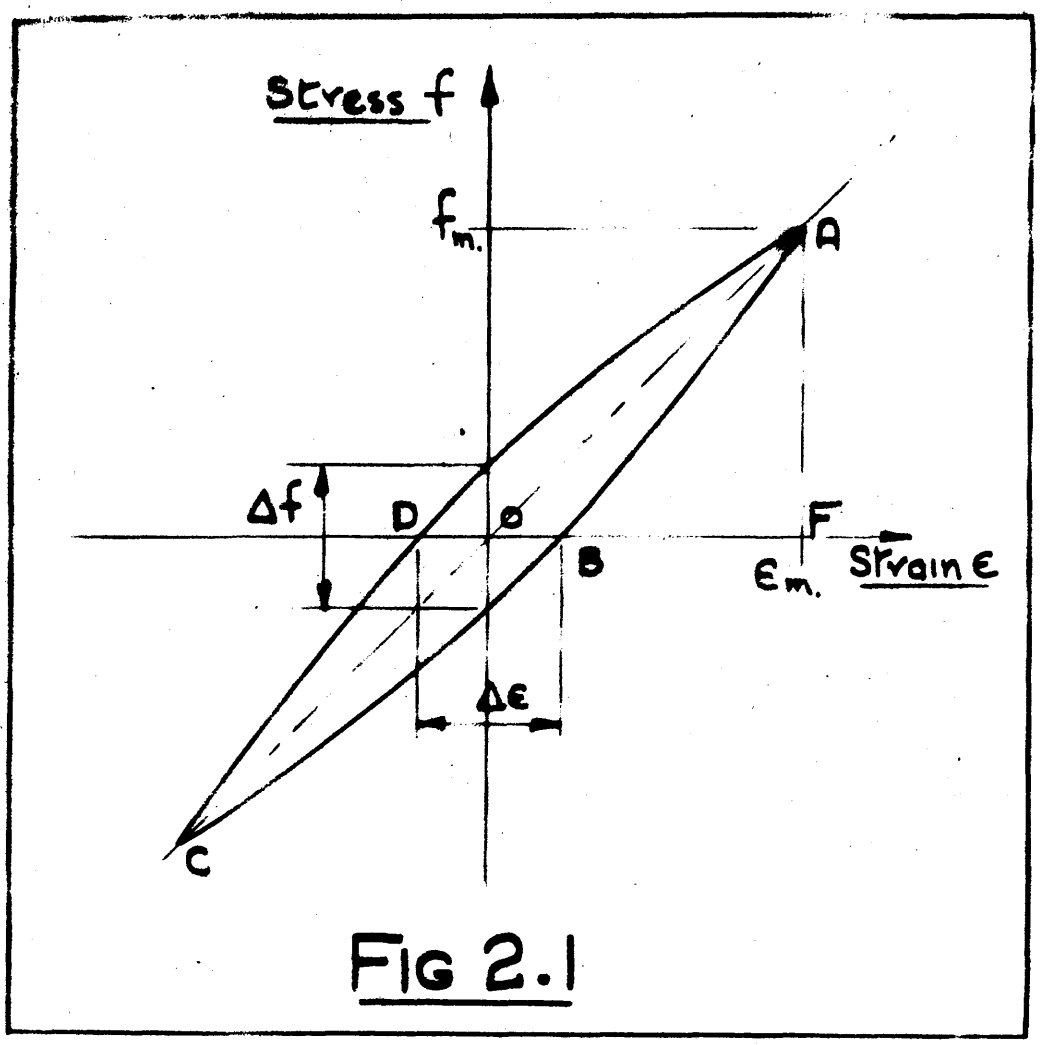

FIG 2.1

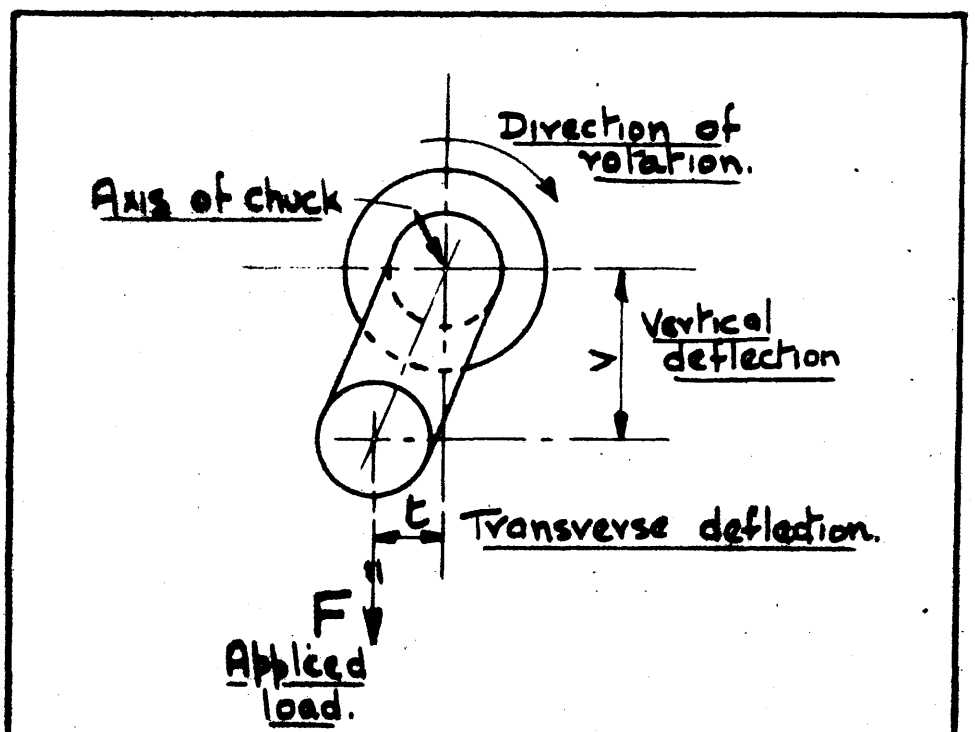

FIG 2.32

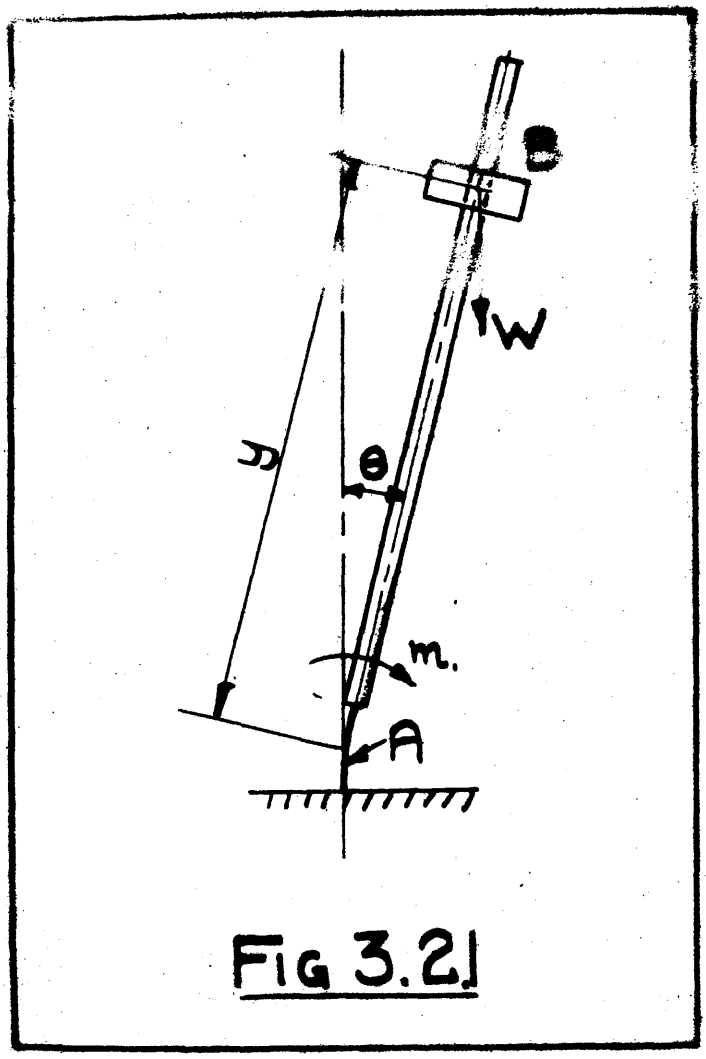

FIG 3.2.1

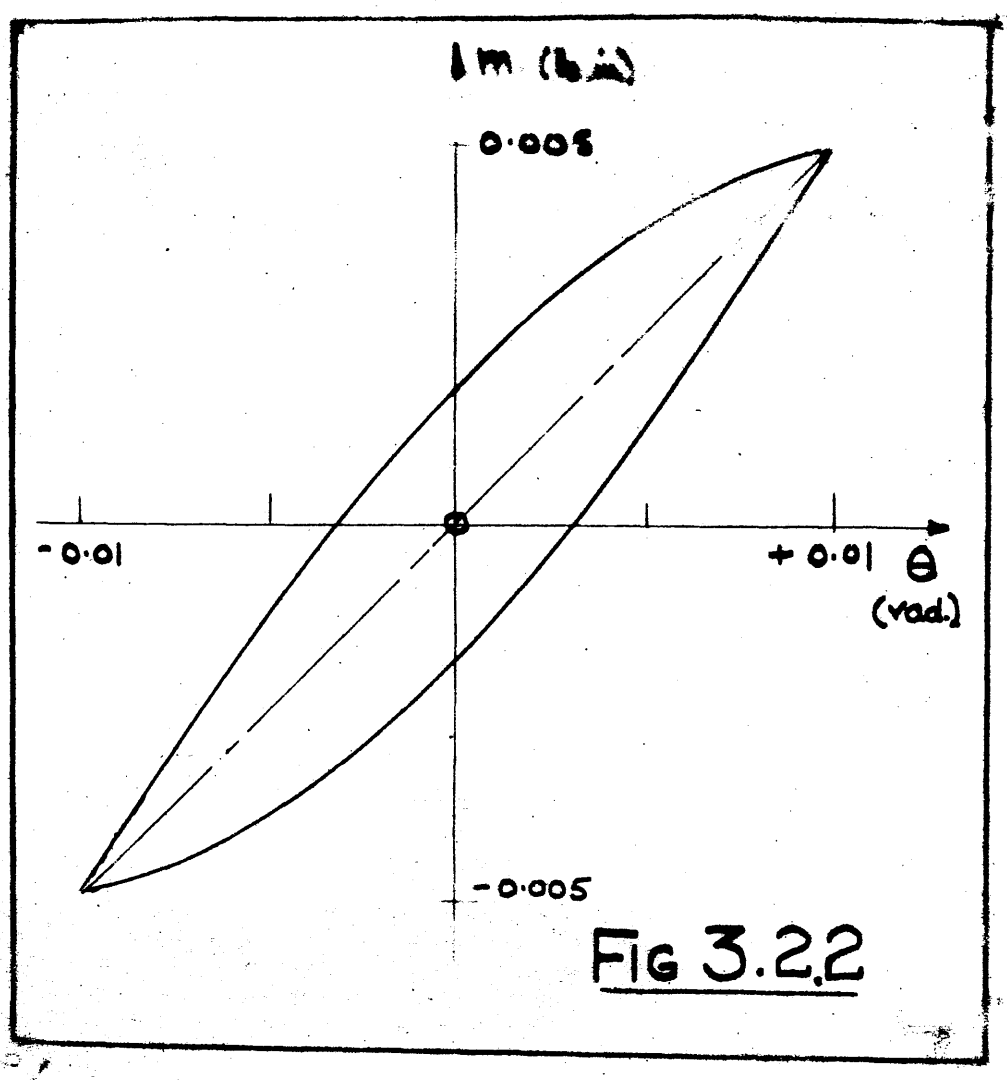

FIG 3.2.2

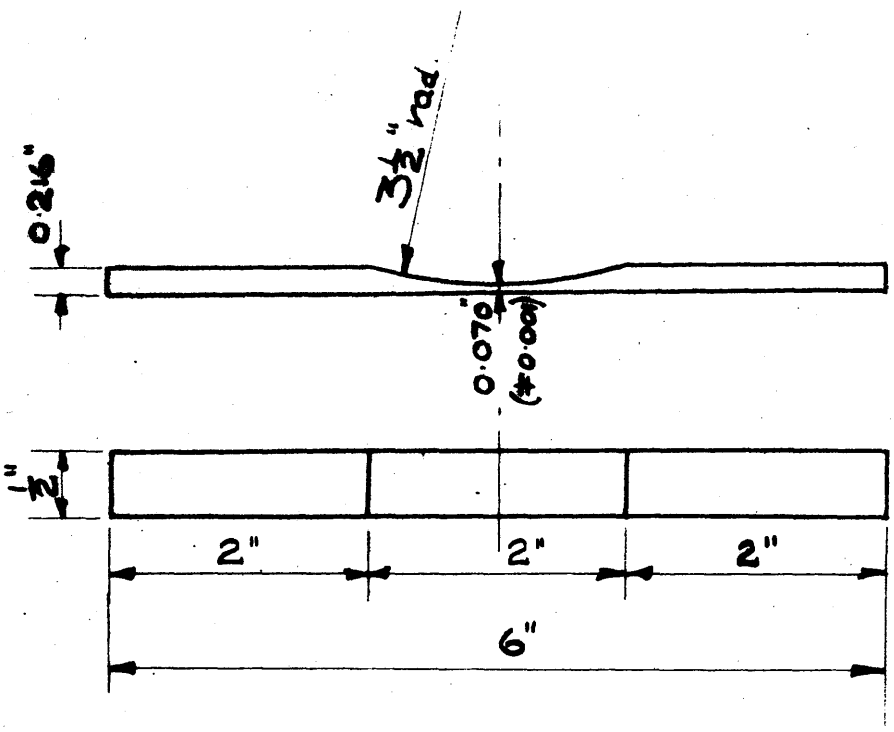

Ground all over except ends.

SPECIMEN FOR DAMPING TESTS.

FIG 3.3

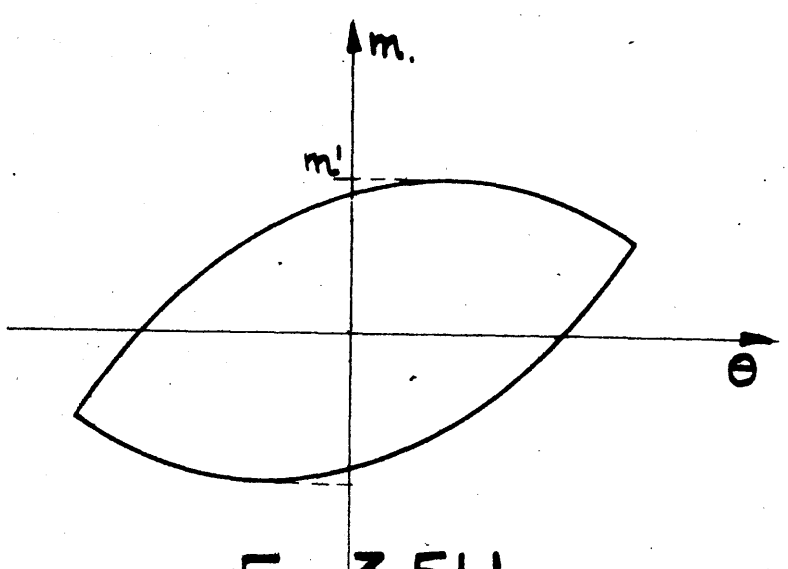

FIG. 3.51.

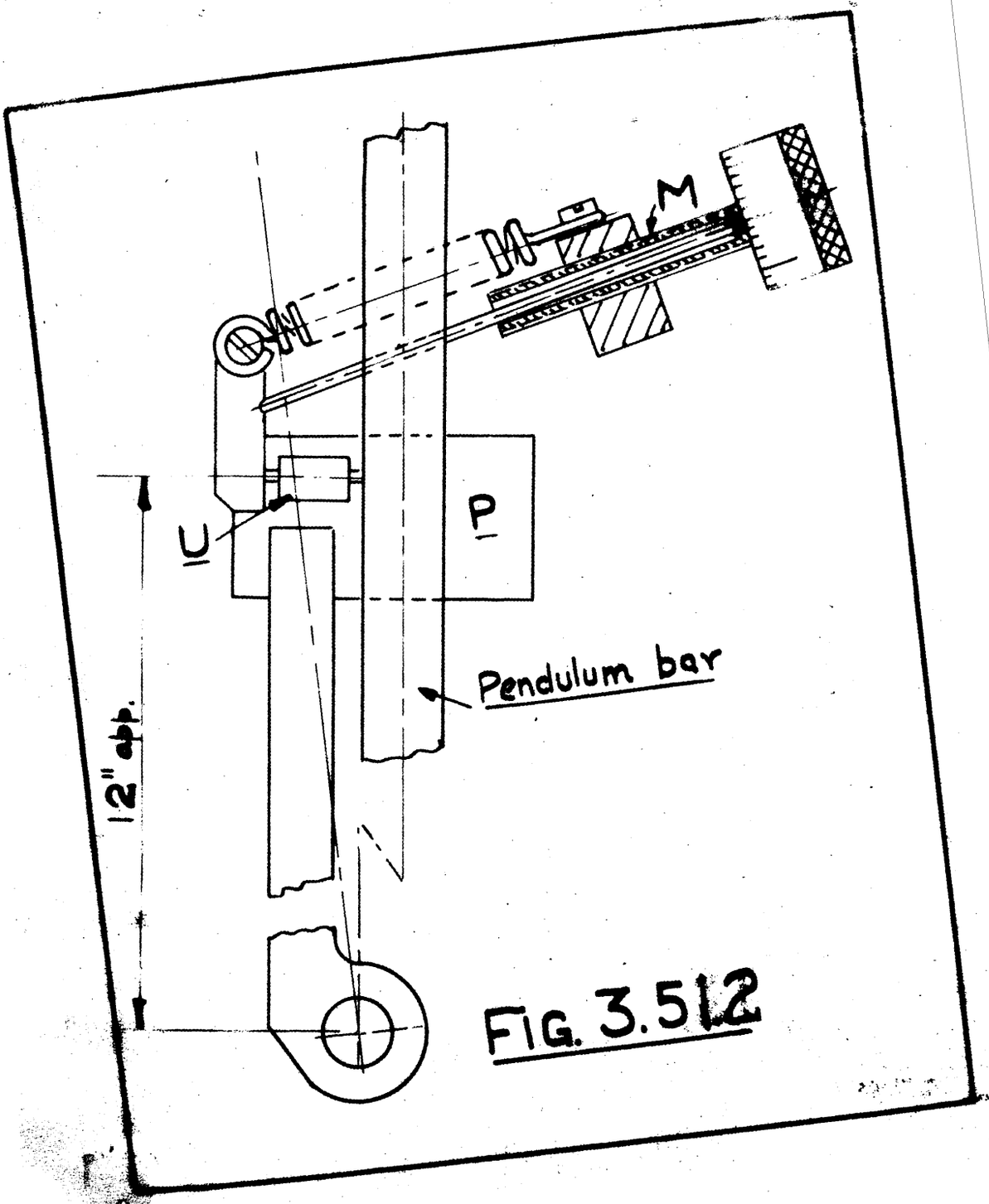

Fig. 3.512

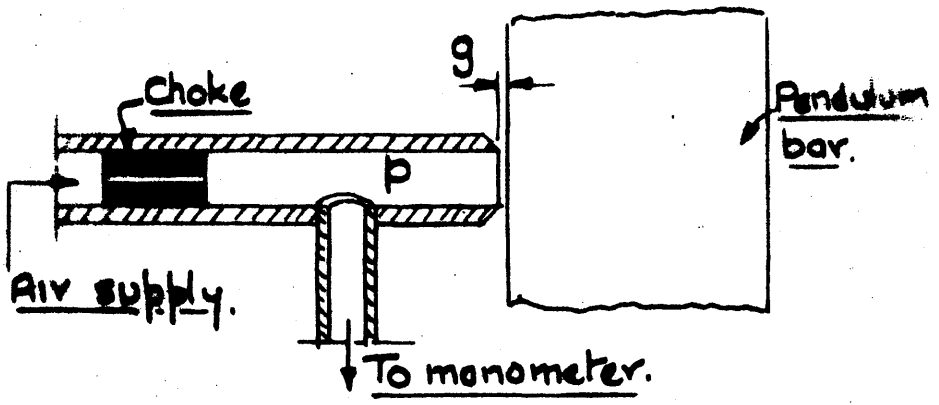

FIG 3.52

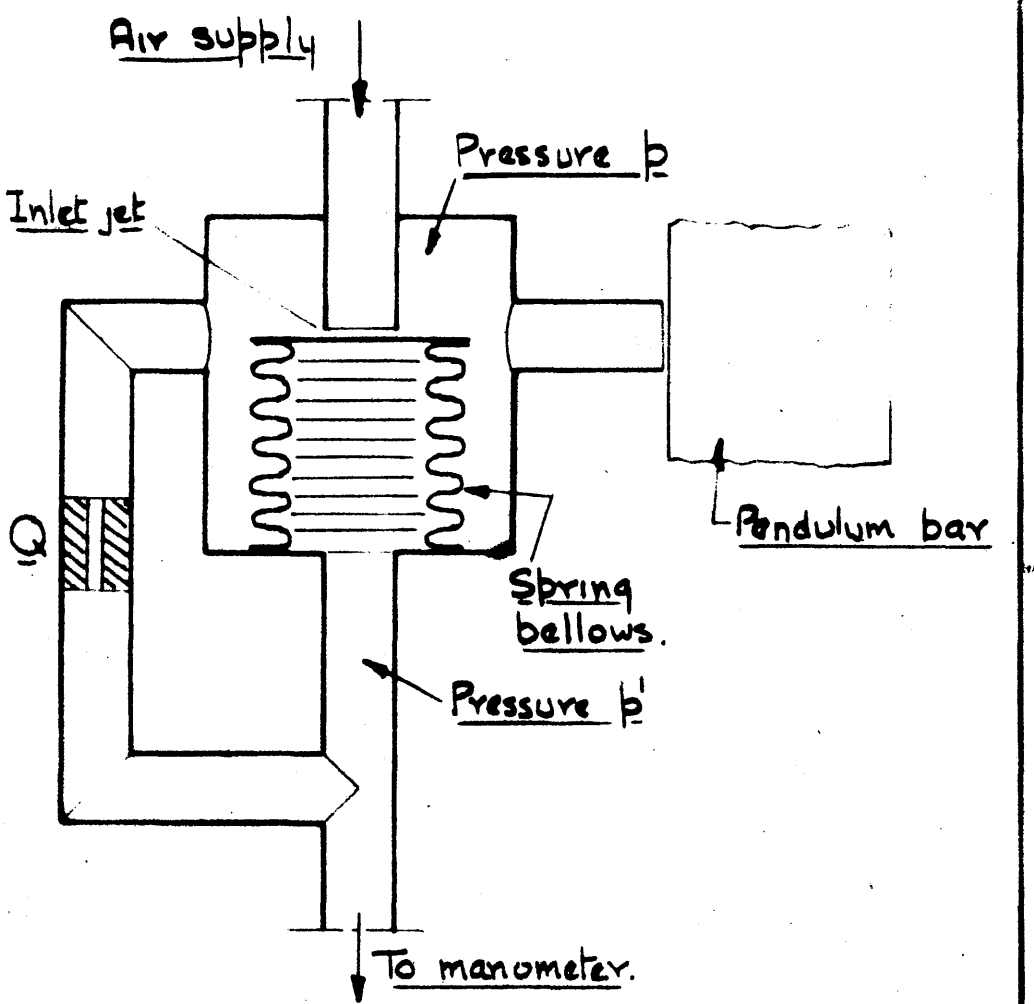

FIG 3.53

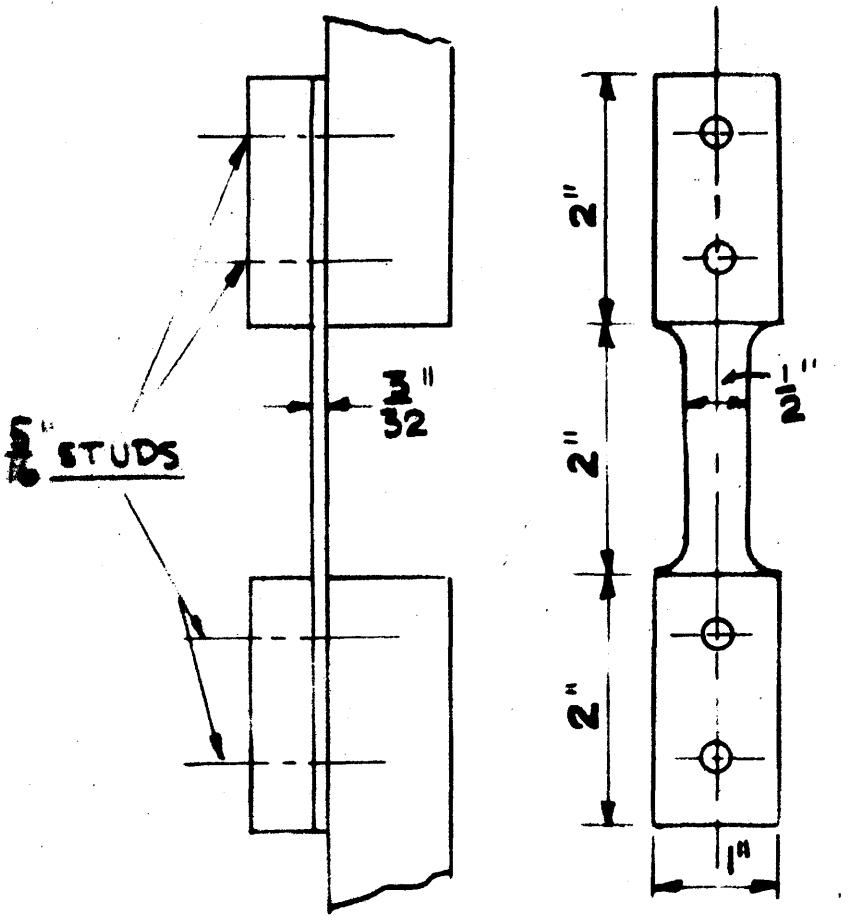

FIG 3.6.1

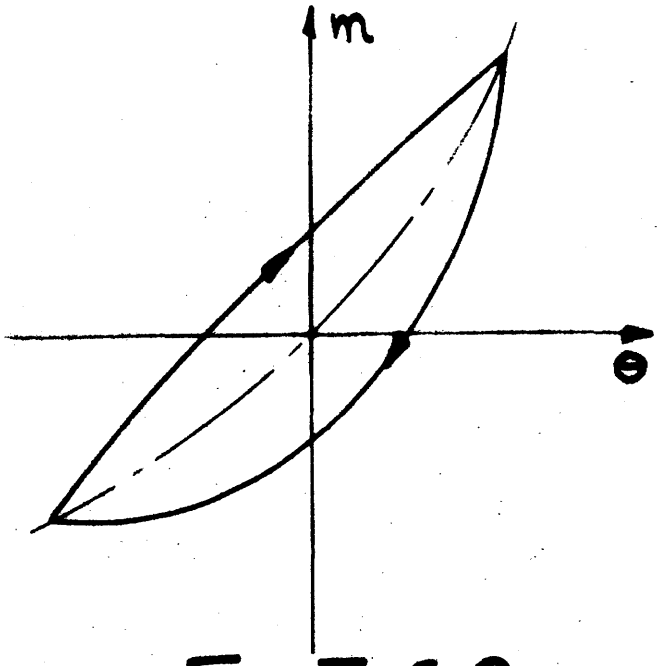

FIG. 3.6.2.

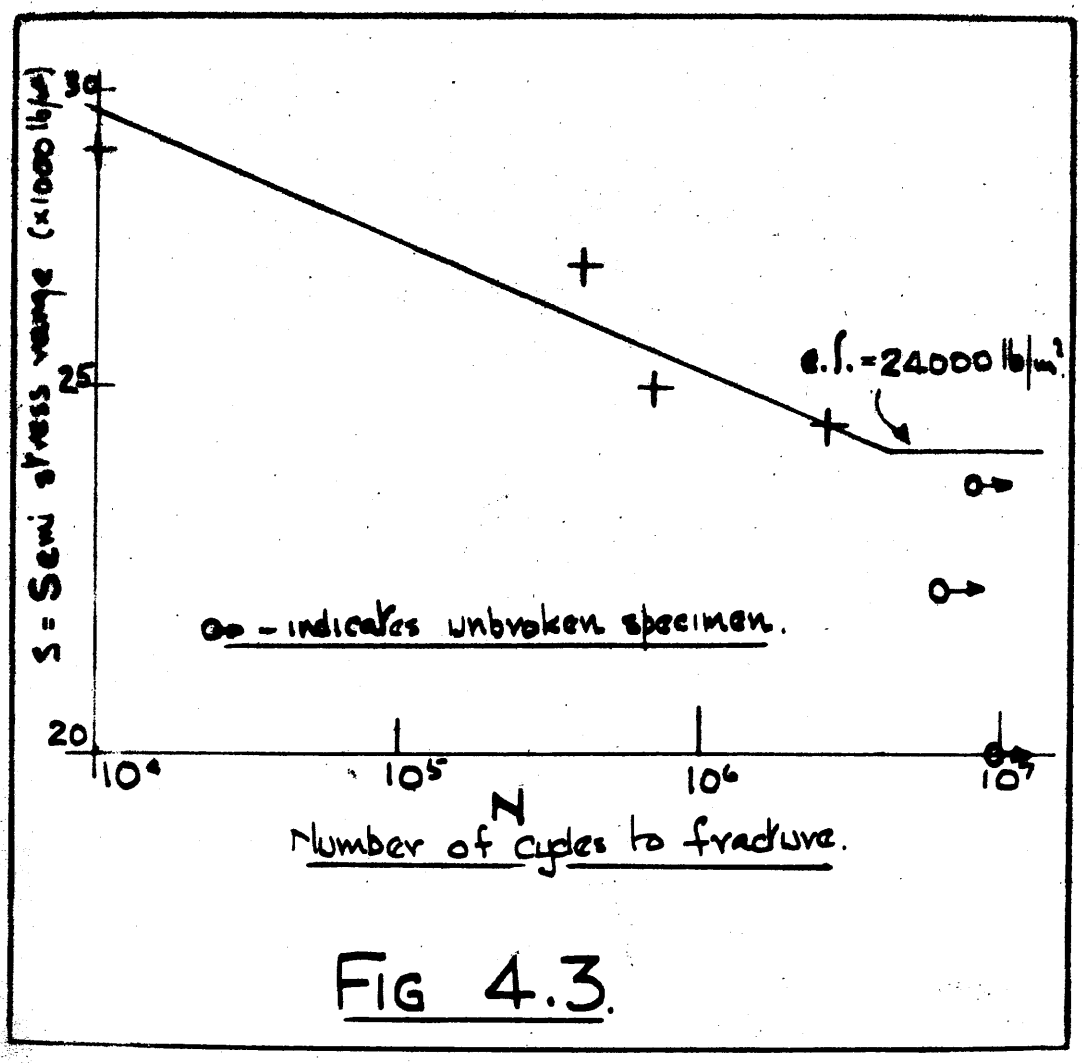
S = Semi stress range (x1000 lb/in²)
30
25
20
e.f. = 24000 lb/in²
o→
o→
o→ - indicates unbroken specimen.
10⁴
10⁵
10⁶
10⁷
N
Number of cycles to fracture.

FIG 4.3.

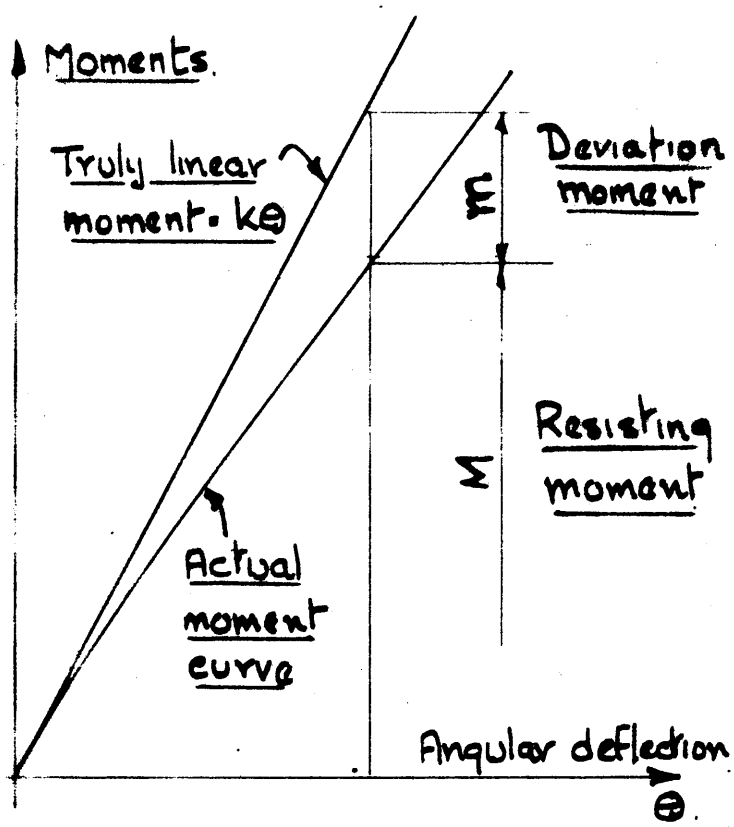

FIG 4.4.1.

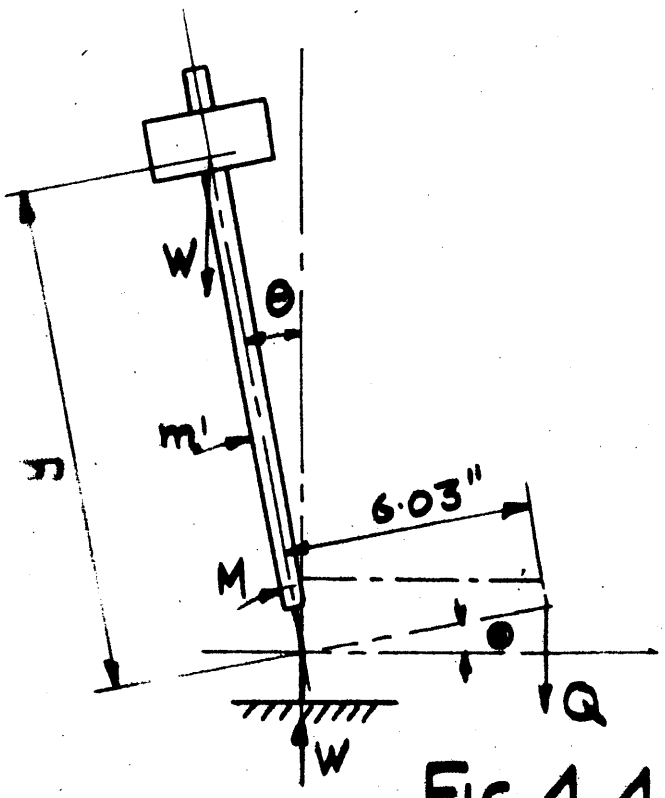

FIG. 4.4.2

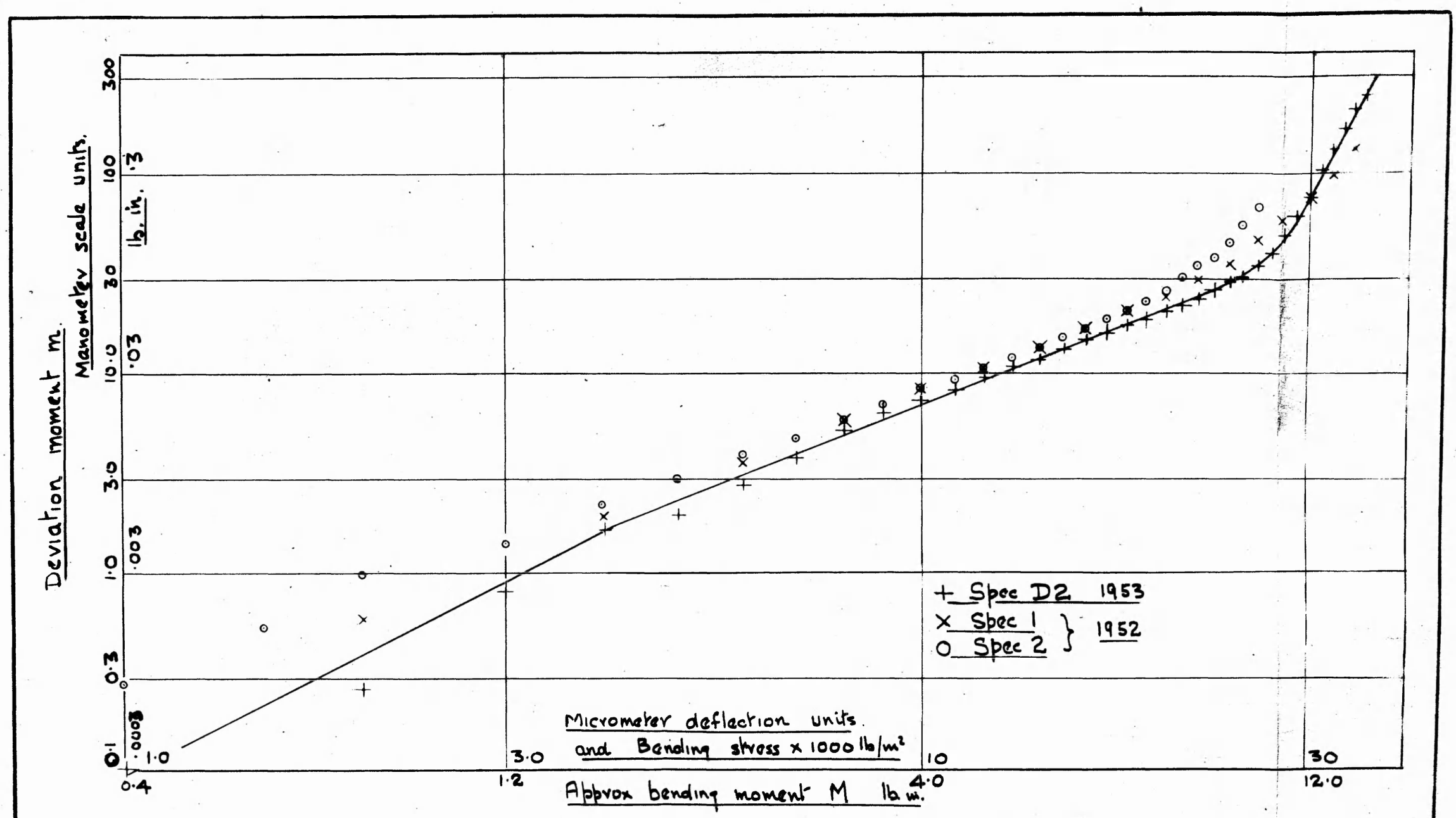

Deflection, stress and total bending moment M.

FIG 4.4.3

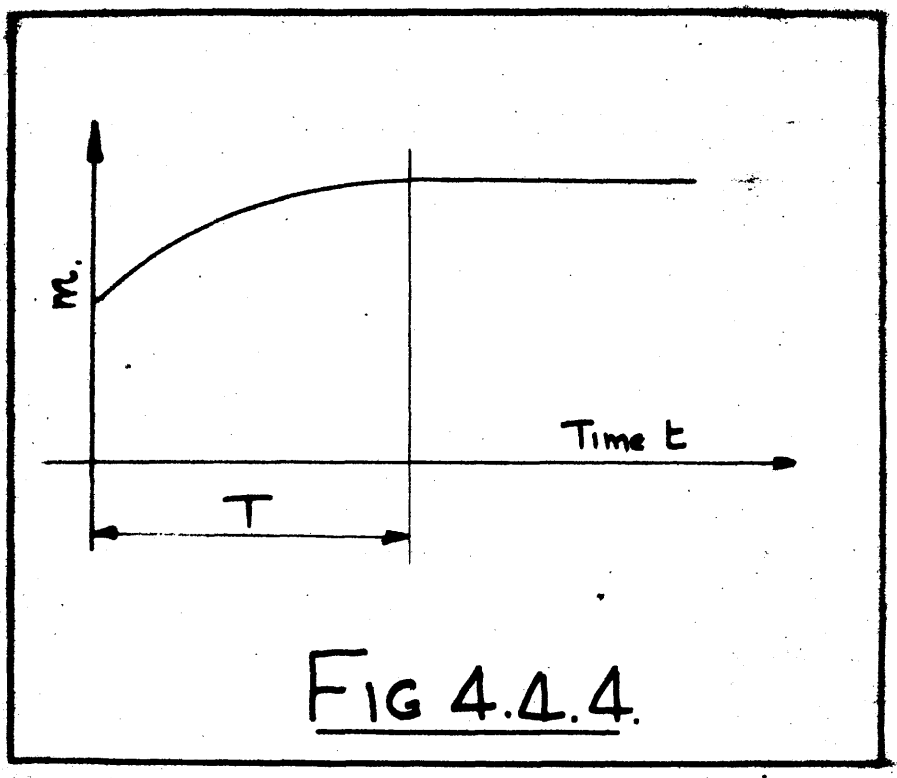

FIG 4.4.4.

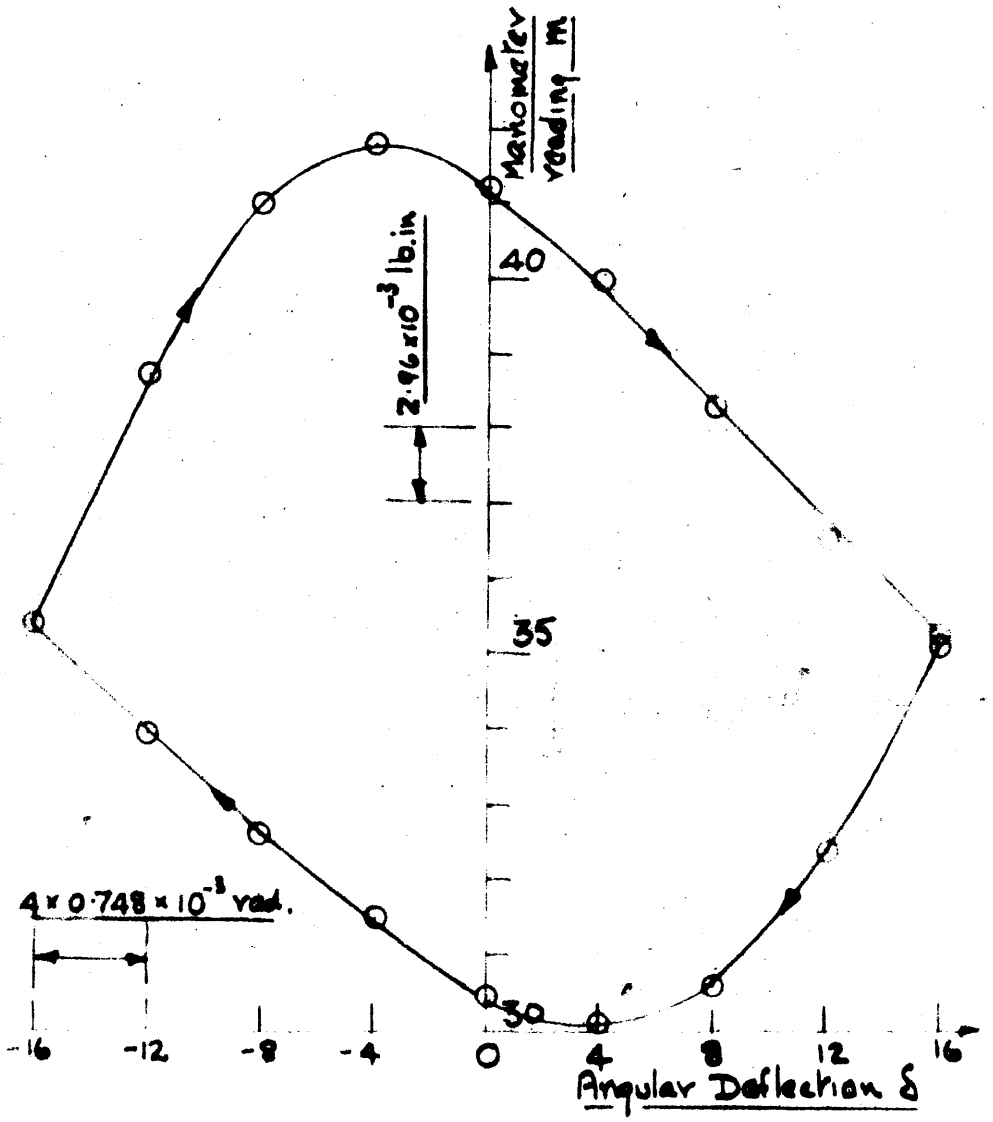

Observed hysteresis loop Spec D3.

Bending stress ≠ 16000 lb/in².

5th cycle of stress.

Loop area = 511 × 10⁻⁶ lb.in

Max. strain energy = 39,800 × 10⁻⁶ lb.in.

Damping coefficient $D = \frac{511}{39800} = 0.0128$

FIG. 4.5.1.

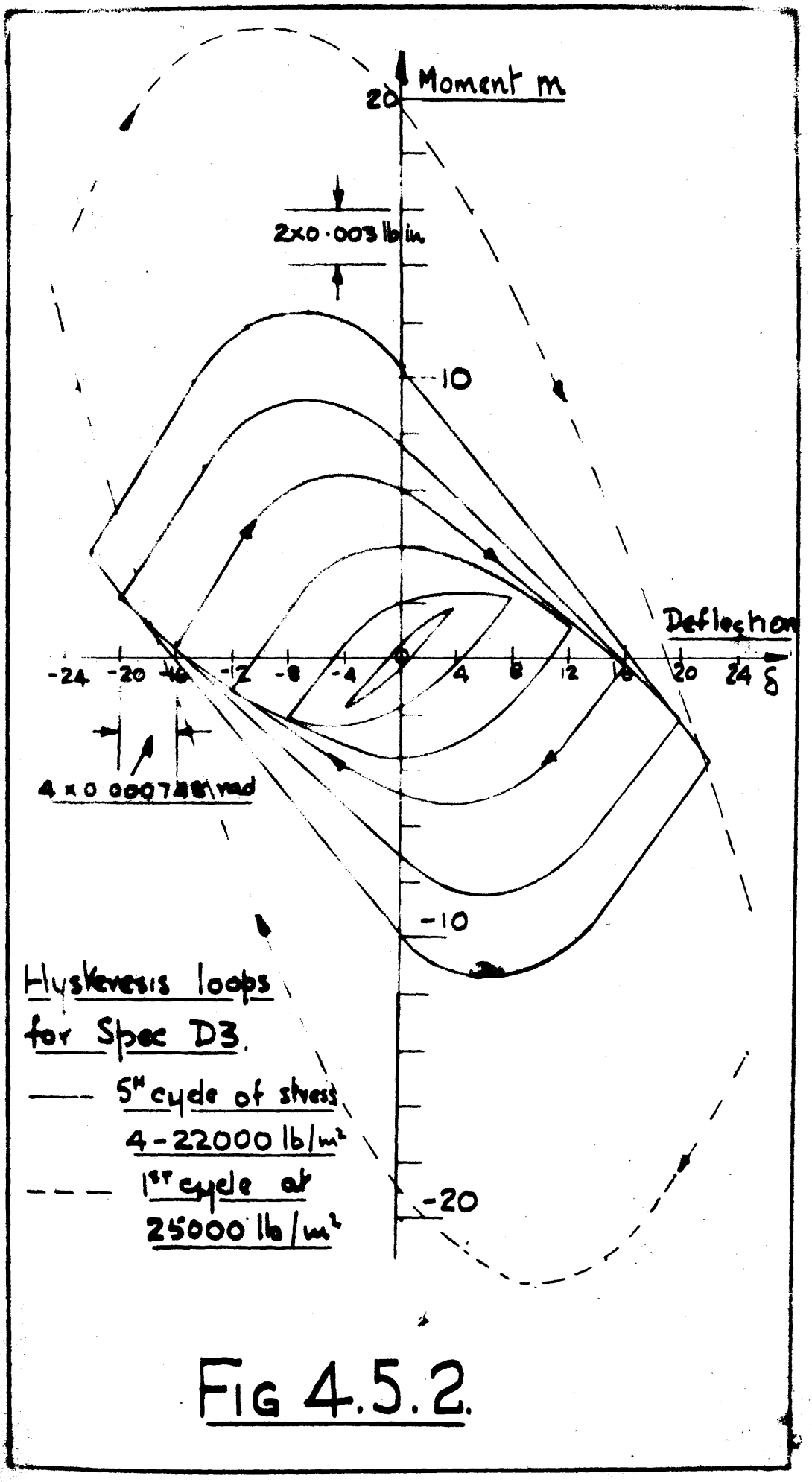
Moment m
20
2x0·003 lb in.
10
-10
-20
Deflection
-24 -20 -16 -12 -8 -4 0 4 8 12 16 20 24 δ
4 x 0 000748 rad
Hysteresis loops
for Spec D3.
5th cycle of stress
4-22000 lb/in²
1st cycle at
25000 lb/in²

FIG 4.5.2.

Table I

Damping coefficients of Specimen D3.

Bending stress lb/in² and Maximum strain energy lb in x 10^{-6}.	Stress cycle.	Energy loss per cycle (loop area) lb in x 10^{-6}	Damping coefficient D.
±4,000	1st	10·41	0·00412
	5	11·09	0·00448
	10	9·2	0·00373
	52	9·8	0·00400
(2,490)	100	12·0	0·00495
±8,000	1st	91·2	0·00922
	5	83·4	0·00840
	10	84·5	0·00853
	50	90·0	0·00910
(9,950)	100	83·0	0·00836
±12,000	1st	256	0·0116
	6	269	0·0121
	10	239	0·0108
	21	246	0·0113
(22,400).	51	246	0·0113
± 16,000	1st	568	* 0·0142
	2	514	0·0128
	5	512	0·0128
(39,800).	10	502	0·0126
±20,000	1st	810	0·0132
	2	845	0·0138
	5	860	0·0140
(62,300)	10	975	0·0159
± 22,000	1st	1170	0·0157
	2	1285	* 0·0172
	5	1295	0·0174
(75,200)	10	1330	0·0178
± 25000	1st	3020	*. 0·0313
	2	large — off scale.	

*. Possibly unreliable values — loops failed to close.

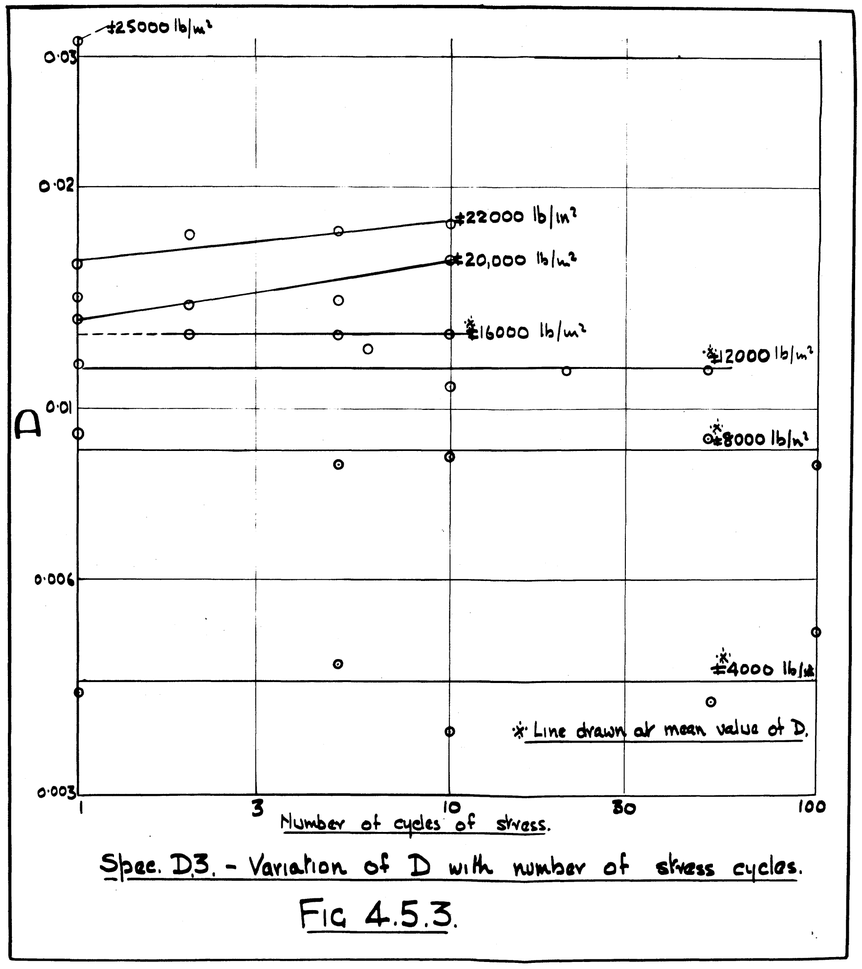

Spec. D3. - Variation of D with number of stress cycles.

Fig 4.5.3.

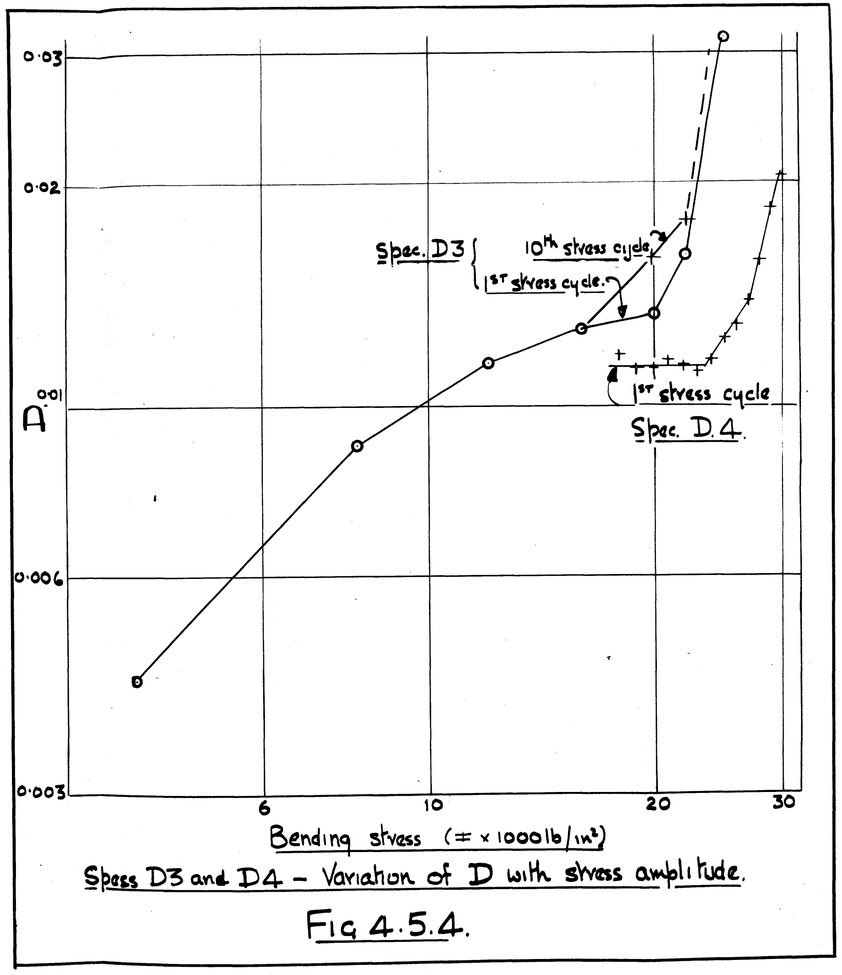

Specs D3 and D4 - Variation of D with stress amplitude.

Fig 4.5.4.

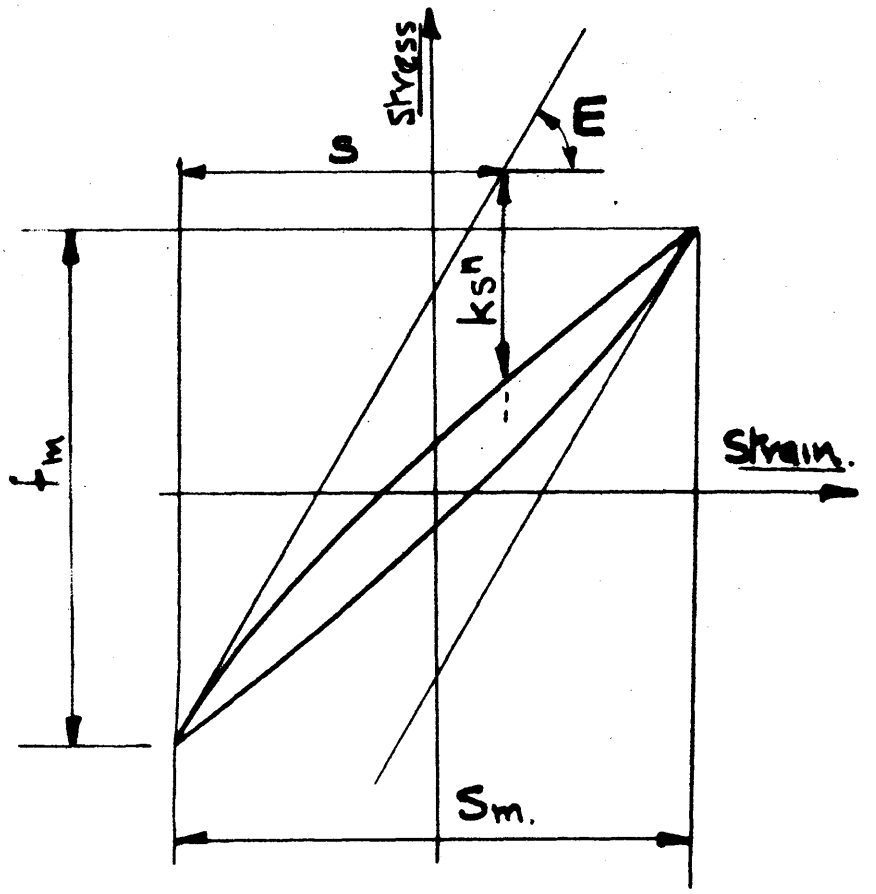

FIG. 5.51

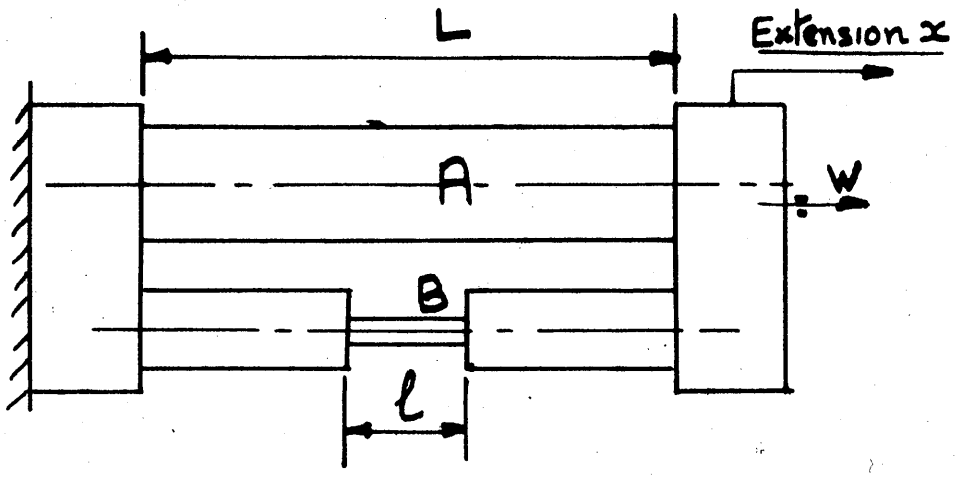

FIG. 5.52.1

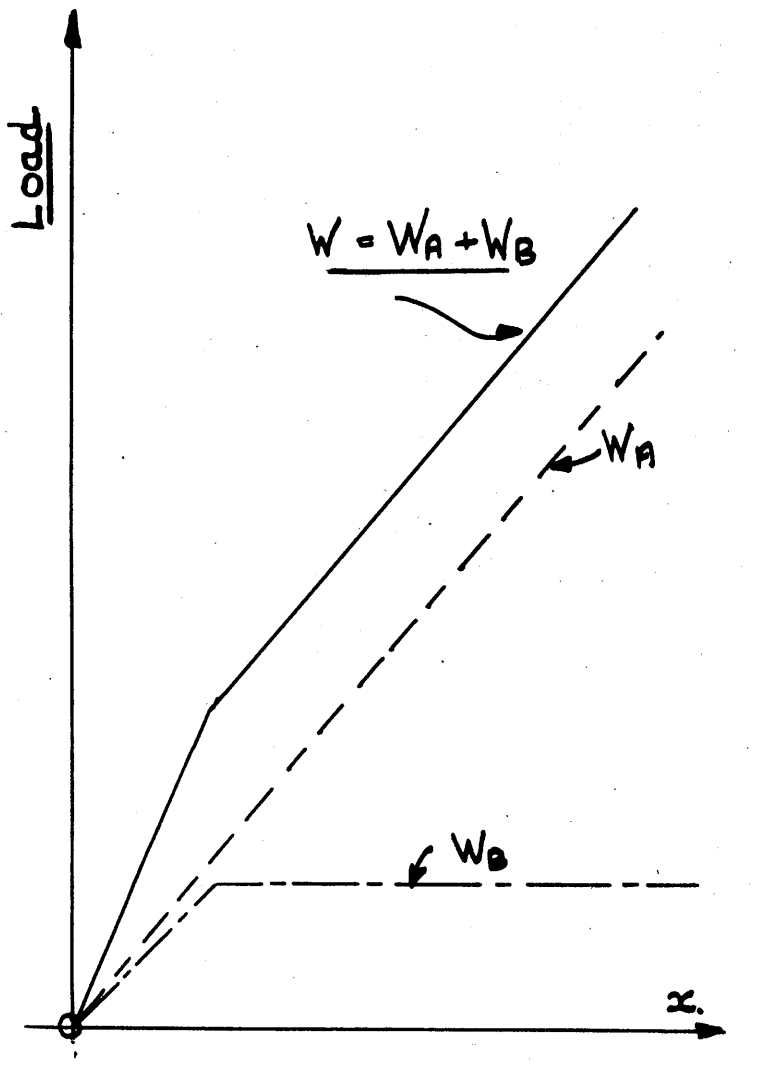

Load-extension diagram for a single loading

FIG. 5.52.2

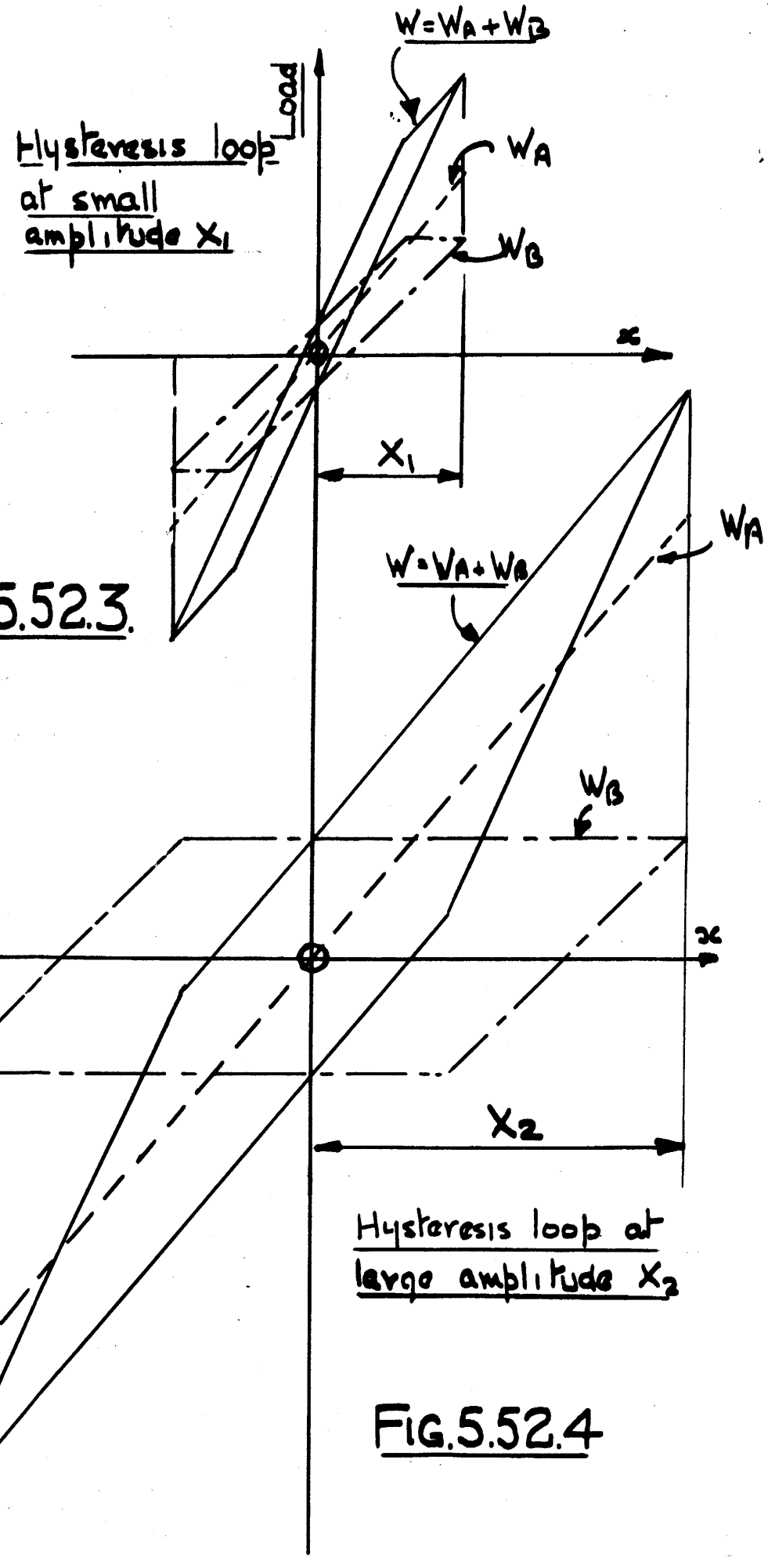

FIG. 5.52.3.

Hysteresis loop at large amplitude X_2

FIG. 5.52.4

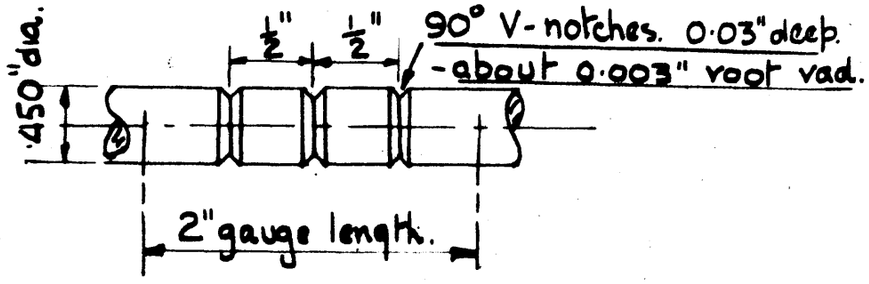

Notched tensile test specimen.

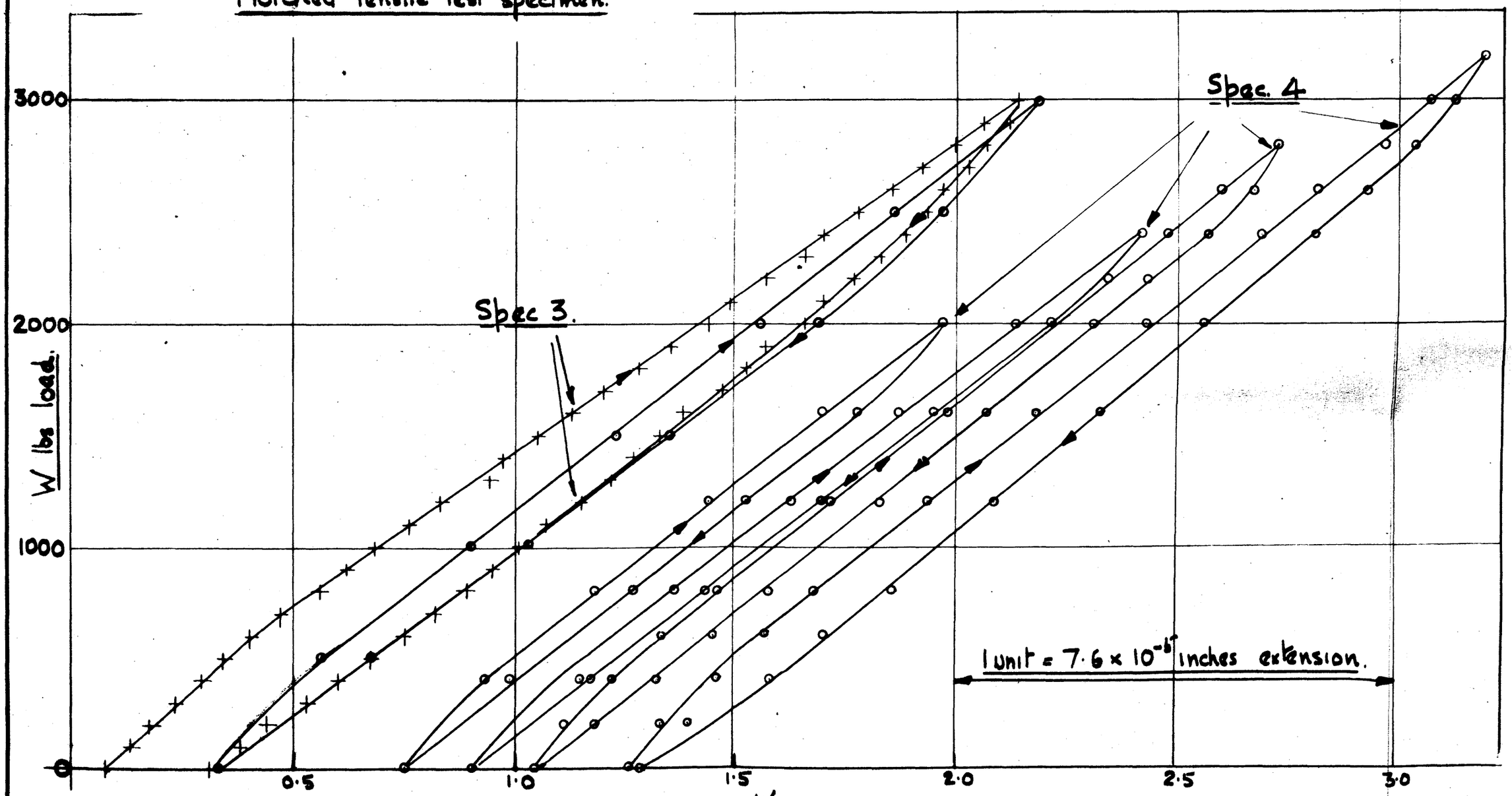

FIG. 5.53

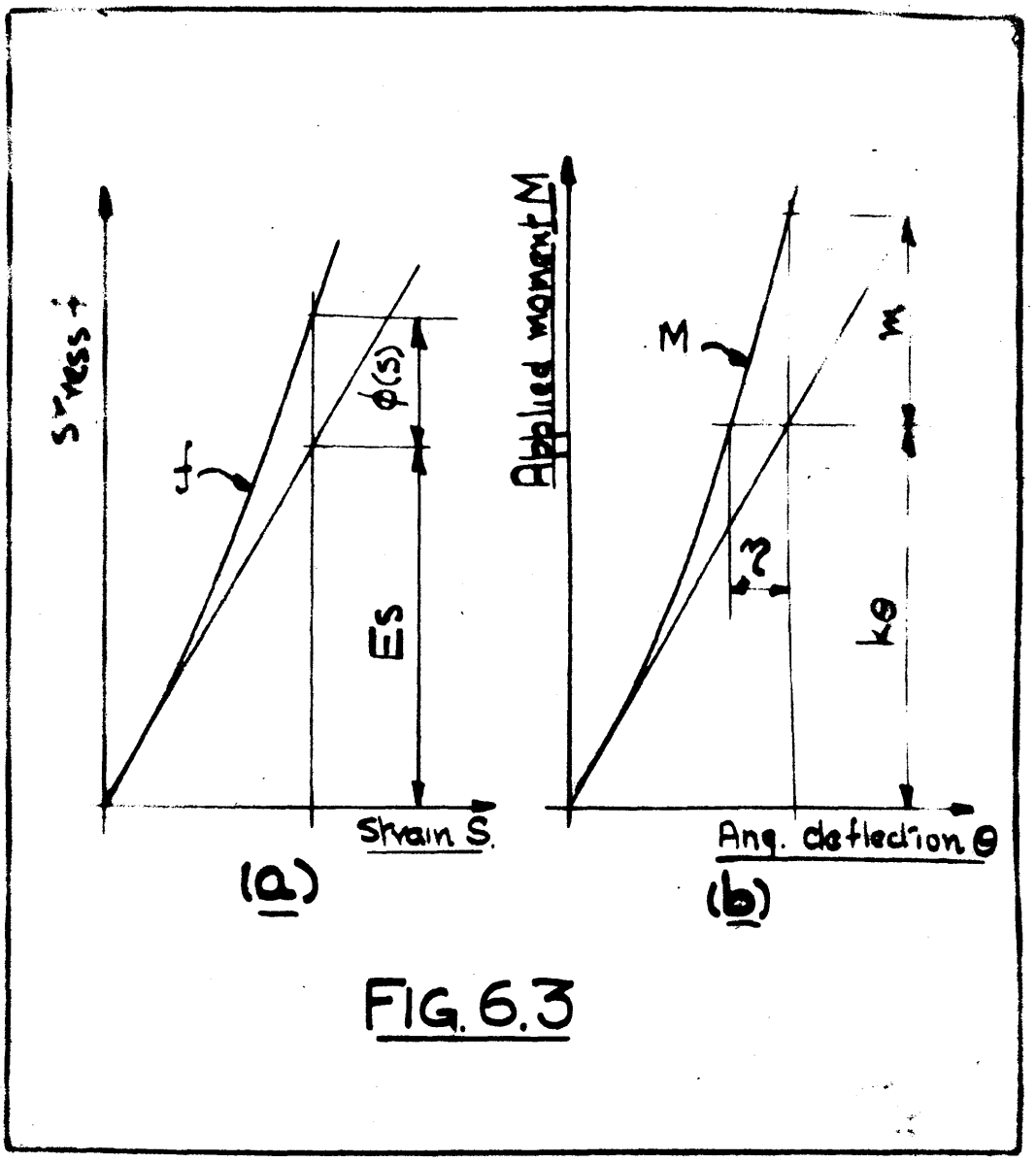
Stress f
f
φ(s)
Es
Strain S
(a)
Applied moment M
M
w
ϑ
kϑ
Ang. deflection ϑ
(b)

FIG. 6.3

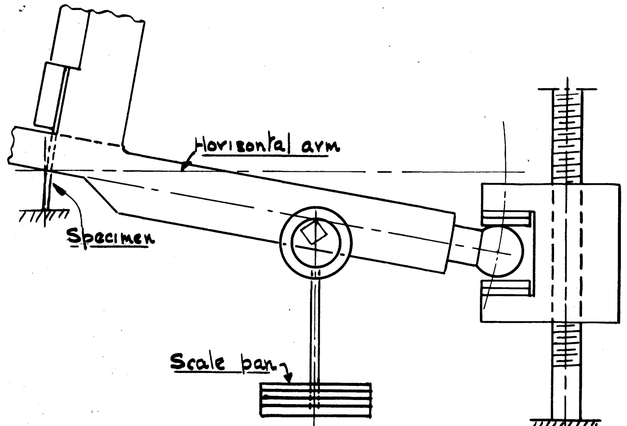

FIG 7.2.

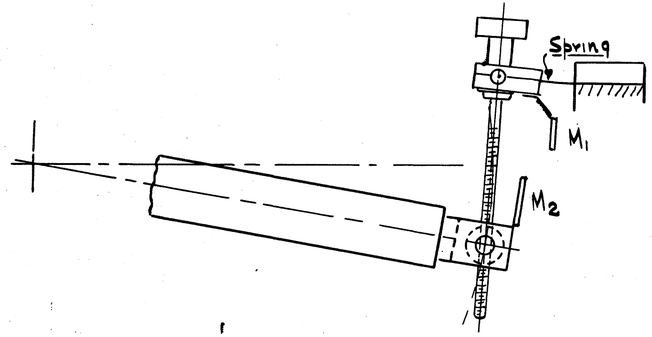

FIG. 7.3.1.

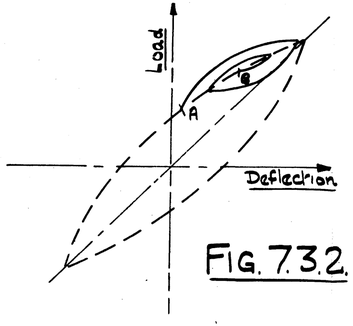

FIG. 7.3.2.

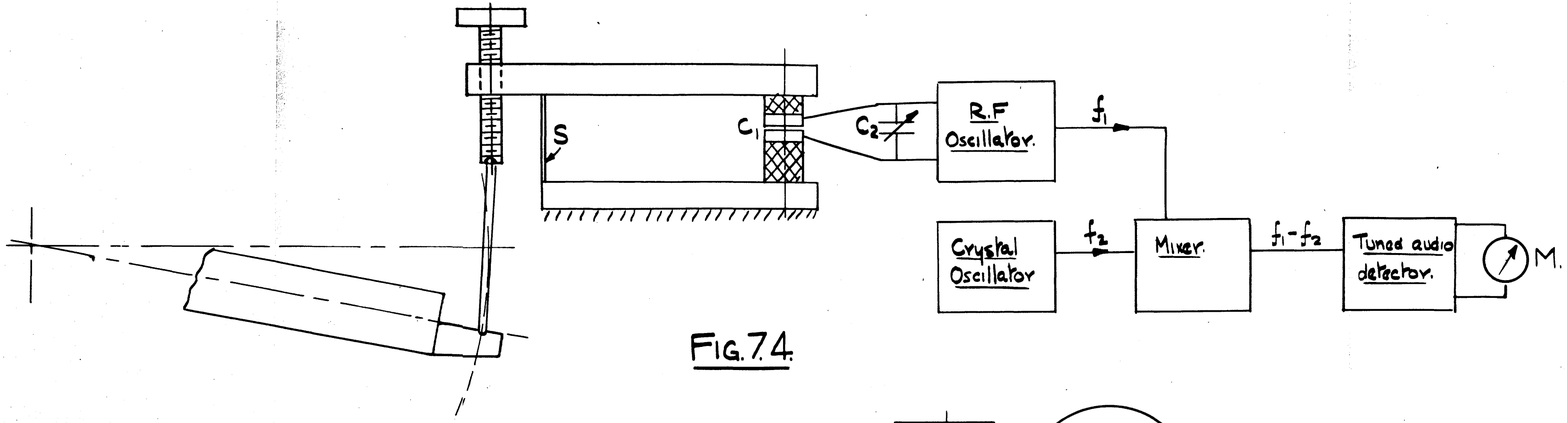

FIG. 7.4.

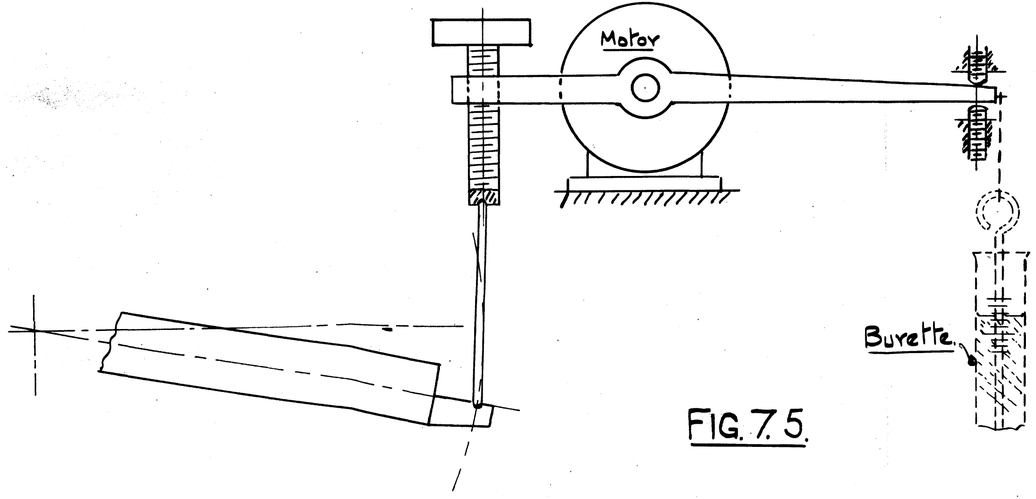

FIG. 7.5.

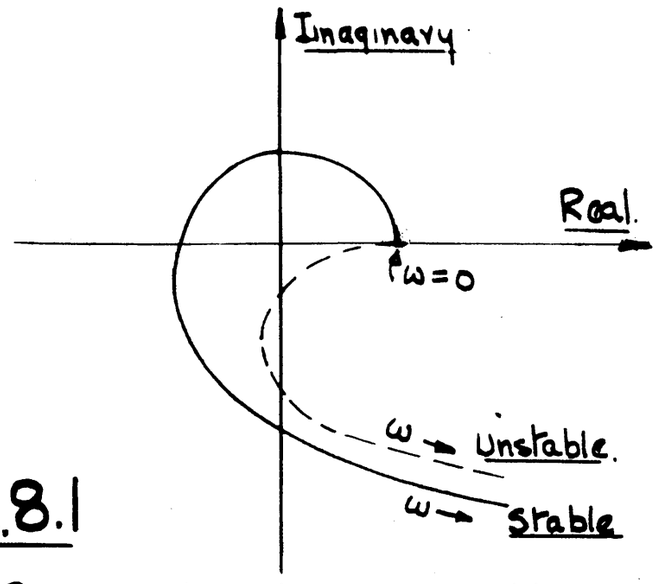

FIG. 8.1

General Leonhard stability diagram.

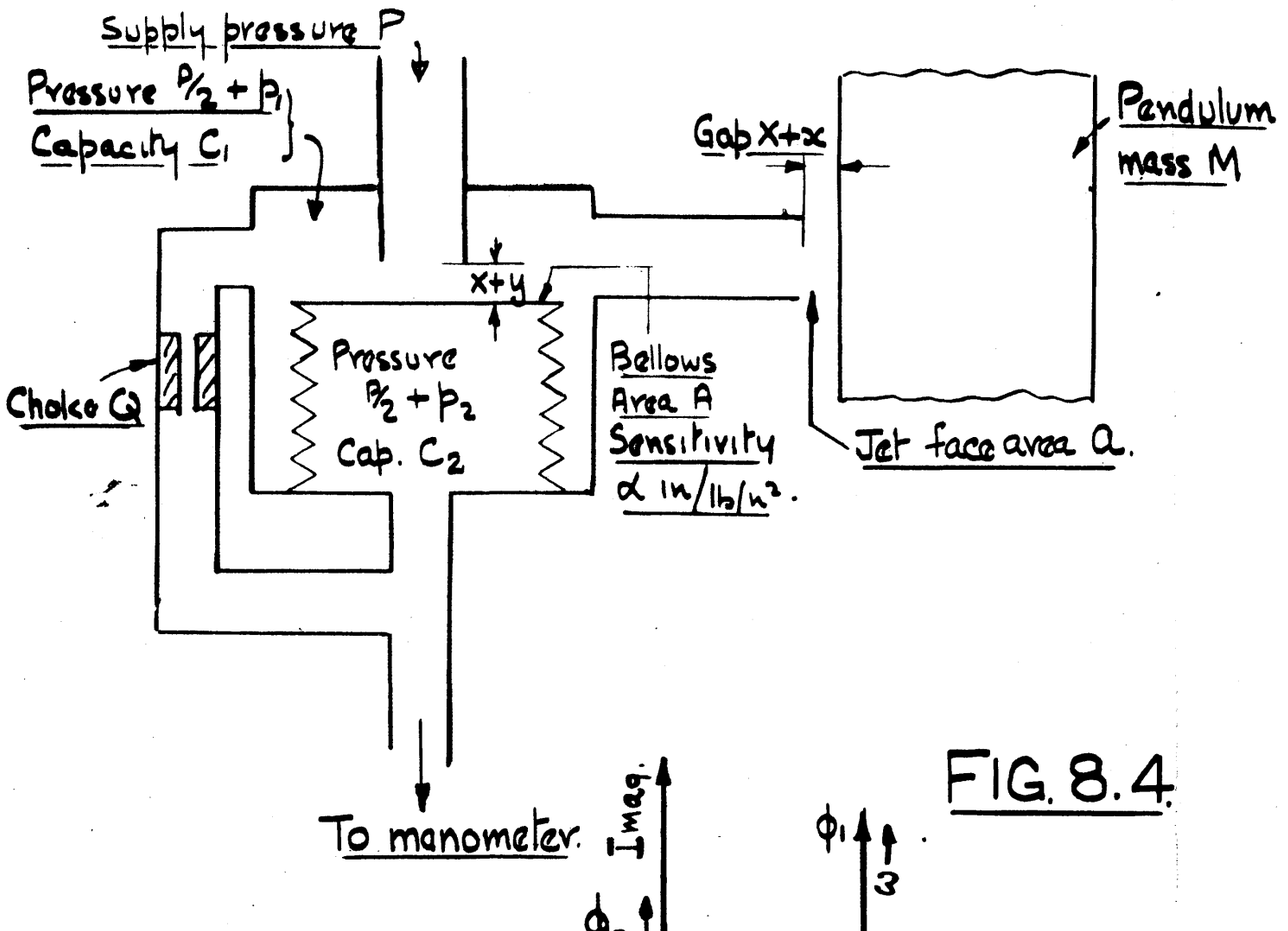

FIG. 8.4

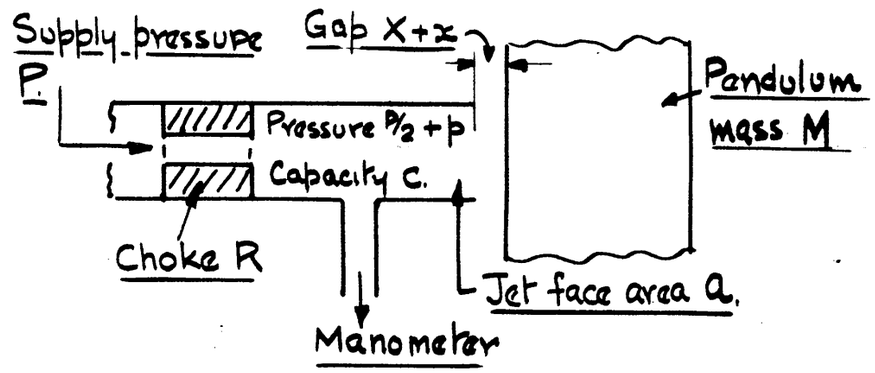

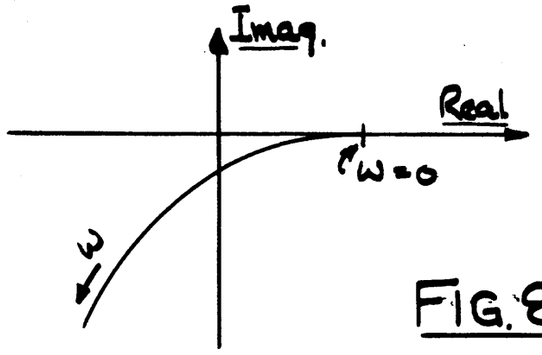

FIG. 8.2

Simple system and corresponding stability diagram.

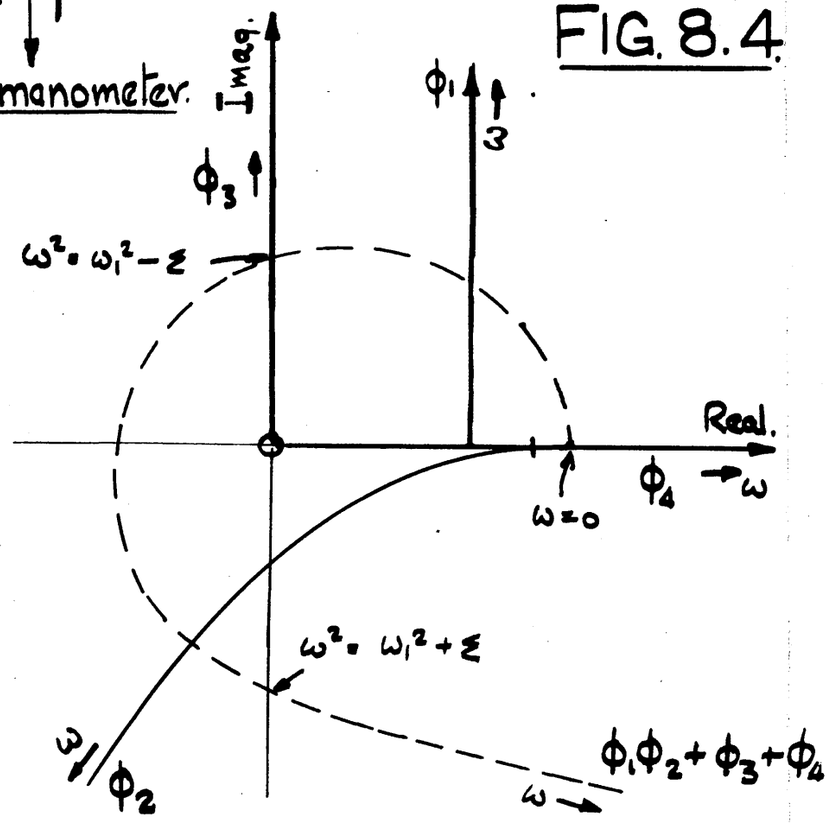

Stabilized system and corresponding stability diagram